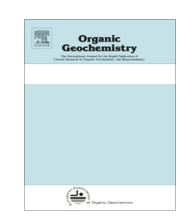


Contents lists available at ScienceDirect

## **Organic Geochemistry**

journal homepage: www.elsevier.com/locate/orggeochem



# Lipid biomarker stratigraphic records through the Late Devonian Frasnian/Famennian boundary: Comparison of high- and low-latitude epicontinental marine settings



Emily E. Haddad <sup>a,\*</sup>, Michael L. Tuite <sup>b</sup>, Aaron M. Martinez <sup>a</sup>, Kenneth Williford <sup>b</sup>, Diana L. Boyer <sup>c</sup>, Mary L. Droser <sup>a</sup>, Gordon D. Love <sup>a</sup>

#### ARTICLE INFO

# Article history: Received 16 February 2016 Received in revised form 1 May 2016 Accepted 12 May 2016 Available online 20 May 2016

Keywords: Upper Kellwasser Black shale Mass extinctions Appalachian Basin Madre de Dios Basin Lipid biomarkers Redox Nitrogen isotopes

#### ABSTRACT

The pervasiveness of black shale preservation in association with Late Devonian biological crises suggests marine anoxia played a major role in driving ecological perturbations. However, Devonian black shale deposition is still mechanistically poorly understood. We have compiled detailed biomarker lipid chemostratigraphic records for 83 different rock samples using molecular constituents of bitumens of Upper Kellwasser equivalent black shales from two foreland basins: from the low paleolatitude Appalachian Basin (New York State) and from the high paleolatitude Madre de Dios Basin (Bolivia), in order to better understand local environmental conditions and organic source inputs during this depositional event. Despite strong indications from stable nitrogen isotopic signatures for fixed nitrogen nutrient limitation, the biomarker assemblages with consistently low-moderate hopane/sterane ratios (<0.8) indicate that algae were major marine primary producers in both basins throughout the Frasnian/ Famennian (F/F) stratigraphic coverage. Consistently higher C<sub>28</sub>/C<sub>29</sub> sterane ratios at higher paleolatitude in the more nutrient-replete Madre de Dios Basin suggest prasinophyte microalgae flourished in this setting in accordance with palynological evidence for high contributions of Tasmanites cysts in these strata. All samples contain only very low absolute amounts of aryl isoprenoids (with 2,3,6-trimethyl substitution) and other aromatic carotenoids, up to several orders of magnitude lower than concentrations reported from other Phanerozoic euxinic basins. These data are consistent with local marine paleoredox models for both basins lacking a persistently shallow sulfidic aquatic zone and demonstrate that temporally persistent or spatially pervasive photic zone euxinia is not necessarily associated with all black shale sequences in the Late Devonian.

© 2016 Published by Elsevier Ltd.

## 1. Introduction

Organic-rich sedimentary rocks are prolific hydrocarbon (oil and gas) sources and, since their occurrences commonly correlate with mass extinction events throughout the Phanerozoic, the geochemical and fossil records preserved in these strata are of central interest to many paleoenvironmental studies (most recently, Lenniger et al., 2014; Rivera et al., 2015; van Helmond et al., 2015). The details of the processes of black shale accumulation, however, are poorly understood and under continual debate (Tyson and Pearson, 1991; Harris, 2005; Tyson, 2005).

The Late Devonian is particularly known for its global abundance of organic-rich sedimentary facies that are associated with biotic events of varying magnitudes (House, 2002). Reconstructing these depositional environments is of particular value and interest to black shale research: unique continental configurations, with much of the continental masses concentrated near the equator (Golonka et al., 1994), coupled with high sea level stands and active orogenesis (notably the Acadian and Antler orogenies of Laurentia; Averbuch et al., 2005), created the ideal conditions for massive epeiric seaways, the loci for organic carbon burial. These global black shale depositional events characteristically occur in association with elevated extinction rates in marine fauna. The bio-event at the Frasnian/Famennian (F/F) stage boundary, the Kellwasser Event (Buggisch, 1991; House, 2002), which correlates with the deposition of the Upper Kellwasser bituminous limestone

<sup>&</sup>lt;sup>a</sup> Department of Earth Sciences, University of California-Riverside, 900 University Ave., Riverside, CA 92521, USA

<sup>&</sup>lt;sup>b</sup> Jet Propulsion Laboratory, California Institute of Technology, 4800 Oak Grove Drive, Pasadena, CA 91109, USA

<sup>&</sup>lt;sup>c</sup> Department of Earth Sciences, SUNY Oswego, 241 Shineman Science Center, NY 13126, USA

<sup>\*</sup> Corresponding author.

E-mail address: emily.haddad@email.ucr.edu (E.E. Haddad).

in Europe and organic rich facies globally, has been recognized as a mass extinction event (Raup and Sepkoski, 1982; McGhee, 1996; Bambach et al., 2004). Furthermore, research on the patterns of extinction, origination, and marine ecological selectivity coincident with black shale deposition in the Late Devonian suggest that the environmental processes driving diversity loss may have differed fundamentally from those mechanisms forcing mass extinction events in the Late Ordovician, Late Permian and Late Cretaceous, because the resultant ecosystem restructuring was distinct in its taxonomic impact and ecological fingerprint (Droser et al., 2000; Bambach, 2006; Alroy, 2008).

Because black shale facies are widely characterized as dysoxic or anoxic, studies of Devonian rocks have traditionally invoked spatially pervasive and temporally persistent marine anoxia as the likely mechanism for these biological perturbations (Joachimski and Buggisch, 1993; Becker and House, 1994; Joachimski et al., 2001: Levman and von Bitter, 2002: Bond et al., 2004). There is a growing body of literature, however, suggesting a wider range of possible preservation and/or depositional conditions for black shales beyond the traditional interpretation of requiring a persistently anoxic water-column (Arthur and Sageman, 1994; Murphy et al., 2000a; Boyer and Droser, 2011; Boyer et al., 2011; Rivera et al., 2015). To better understand the range of environments in which black shales can be deposited and to reconstruct the settings for Devonian ecological perturbations, this study examines the microbial ecology and, to a lesser extent, the marine redox chemistry of two Late Devonian basins preserving Frasnian/Famennian black shale.

This study focuses on characterization of the lipid biomarker assemblages in bitumens for a large suite of oil window-mature Late Devonian rocks traversing the Upper Kellwasser Event of the Frasnian/Famennian extinction, from both high and low paleolatitude marine settings. Lipid biomarkers can yield valuable information pertaining to the origins of source organisms (particularly the assemblages of microbial aquatic primary producers which generally account for a high proportion of the biomarker signals in marine paleoenvironments), the thermal maturity of the host organic matter, and the paleoenvironmental conditions (redox, salinity, etc.) in the water column. Hopane/sterane ratios provide a broad but informative measure of bacterial/eukaryotic source inputs which can be compared with a large dataset for source rocks and oils of different geological ages, while sterane carbon number patterns reveal important insights about the major groups of marine algae functioning as important primary producers during Devonian time. Redox sensitive biomarkers, like pristane/phytane ratios and the aromatic carotenoid pigment molecule derived from lipids of green sulfur bacteria, isorenieratane, provide molecular evidence for the occurrence and persistence of anoxia and photic zone euxinia in the Late Devonian

We also measured elemental ratios, including C, N and P, and stable carbon and nitrogen isotopic signatures to gauge important information about local redox conditions and nutrient cycling since microorganisms are the primary mediators of biogeochemical processes, and the relative abundances of eukaryotes and prokaryotes may drive disruptions to ecosystem functions linked to extinction events. For example, nitrogen cycling will differ significantly in an environment dominated by diazotrophic prokaryotes rather than algae, with important implications for primary production, trophic web dynamics and organic matter preservation. These data, in concert with the lipid biomarker stratigraphic record, illuminate the similarities and differences between the low-latitude Appalachian Basin and the high-latitude Madre de Dios Basin during the deposition of the Upper Kellwasser black shale at the Frasnian/Famennian boundary and highlight the marine ecological signatures characteristic of this turnover event.

#### 2. Material and methods

#### 2.1. Geological and sedimentological setting

This study characterizes depositional conditions of black shale deposits from the low-latitude Appalachian Basin of Laurentian (present-day New York State) and the high-latitude Madre de Dios Basin of Gondwana (present-day Bolivia). During the Late Devonian, the Appalachian Basin was situated in the sub-tropics (approximately 30 °S latitude), while the Madre de Dios Basin was at approximately 60 °S latitude (Scotese and McKerrow, 1990; Fig. 1), making a comparison between these two basins useful for insights into potential latitudinal effects on depositional environments.

During the Devonian, the Appalachian Basin was a foreland basin associated with the Acadian Orogeny. Today it contains numerous localities with well-exposed, continuous successions that are biostratigraphically well-constrained and paleontologically well characterized (Thayer, 1974; Woodrow and Isley, 1983; Kirchgasser et al., 1988; Brett et al., 1991; Baird et al., 1999; Sageman et al., 2003). Strata in western New York State preserve the distal expression of the westward thinning package of primarily clastic sediment that was sourced from the Acadian highlands to the west. A thin black shale interval, the Point Gratiot Bed. contained within the Hanover Formation of the Iava Group has been shown to correlate with the global Upper Kellwasser Event (Over, 1997, 2002; Over et al., 2013). The Frasnian/Famennian boundary, defined by the contact of the Upper linguiformis and Lower triangularis conodont chronozones, crops out as a minor disconformity near or at the top of the Point Gratiot Bed.

The four localities sampled for this study are, from most distal to most shoreward, Walnut Creek, Eighteenmile Creek, Irish Gulf and Beaver Meadow Creek (Fig. 1). The Hanover Formation at these localities is underlain by the Pipe Creek Formation, interpreted to represent the Lower Kellwasser Event, overlain by the petroliferous Dunkirk Shale, and is comprised of over 35 m of alternating graygreen mudstones and laminated black shales with nodular carbonate beds, that has been interpreted as an overall shallowing upward succession, with the black shales representing episodic deepening events (Over, 2002). Samples from these localities were hand sampled continuously through the Upper Kellwasser black shale bed; care was taken to collect the least weathered samples, usually along creek beds, and samples were stored in aluminium foil and paper or cloth bags to avoid introducing hydrocarbon contaminants. The Point Gratiot Bed ranges from 19-68 cm thick across the basin: for ease of comparison between the four localities, Figs. 2-4 show an idealized combined stratigraphy, standardizing stratigraphic biomarker trends from each locality to 25 units. Geochemistry of the Upper Kellwasser interval at Walnut Creek, Irish Gulf and a third site not examined as part of the current study, Perry Farm, are reported in Tuite and Macko (2013).

The Madre de Dios Basin in the Devonian is interpreted to be a deepening prodelta that, because of high organic carbon content and dominant kerogenous facies, was thought to have experienced permanent or intermittent anoxia as a result of restriction or stratification. The latest Devonian interval from the Madre de Dios Basin was sampled from the Pando X-1 core, one of five boreholes drilled into the Bolivian Shield, which recovered a sedimentary succession from Precambrian basement rock to the Tertiary (Peters et al., 1997a). Upper Kellwasser equivalent samples were taken from material from the Tomachi Formation, which is poorly biostratigraphically constrained especially in comparison to Appalachian Basin sections, across a 20 m section spanning the Frasnian/Famennian boundary transition. Attempts to assign the Frasnian/Famennian boundary to a single horizon have proven

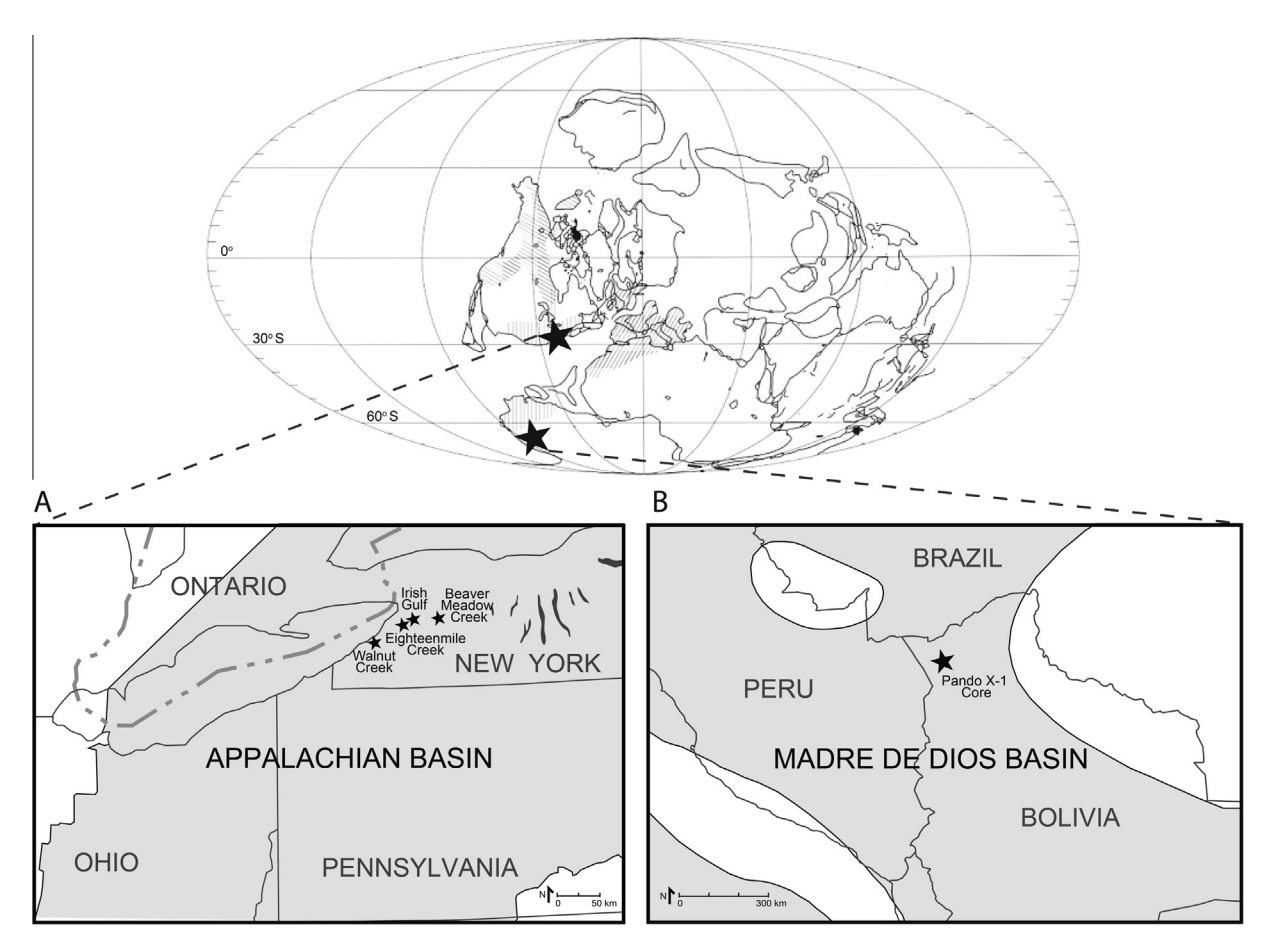


Fig. 1. Locality map: Paleogeography from Scotese and McKerrow (1990). Shaded regions in basinal maps show Devonian extent of the respective epeiric seaways (Appalachian Basin from Swezey (2002); Madre de Dios Basin from Peters et al. (1997a)); non-shaded region is land. Stars indicate sampling localities: in the Appalachian Basin, localities become more distal toward the west.

challenging, and extensive conodont studies have succeeded only in constraining the boundary to a 10 m section (denoted as the F/F interval in Figs. 2–4 and Fig. 6; Over et al., 2009). The very high total organic carbon (TOC) content of these rocks has been proposed to result from enhanced productivity caused by upwelling of nutrients at high latitude (Peters et al., 1997a).

## 2.2. Extraction and separation

For biomarker analysis, the two sample sets were extracted and fractionated in separate labs, with the Appalachian Basin samples extracted and fractionated in the Love Lab at UC Riverside, and the Madre de Dios Basin core samples extracted and fractionated at the University of Virginia. Rock pieces were first trimmed with a water-cooled rock saw to remove outer weathered surfaces and to expose a solid inner portion and sonicated in a sequence of ultrapure water, methanol, dichloromethane (DCM), and hexane before a final rinse with DCM prior to powdering and bitumen extraction. Rock fragments were powdered in a zirconia ceramic puck mill in a SPEX 8515 shatterbox, cleaned between samples by powdering two batches of fired sand (850 °C overnight) and rinsing with the above series of solvents. For each of the Appalachian Basin (NY) samples, 5 g of crushed rock was extracted in a CEM Microwave Accelerated Reaction System (MARS) at 100 °C in a 9:1 DCM:MeOH (v/v) mixture for 15 min. 6-15 g of ground material from the Madre de Dios samples was Soxhlet extracted for 48 h in a mixture of DCM and MeOH (7.5:1, v/v). All solvents were distilled prior to use. Substantial amounts of indigenous bitumen extract were obtained by solvent extraction of these rocks (Tables 1 and 2). Full laboratory procedural blanks with combusted sand were performed in parallel with each batch of rocks to ensure that any background signals were negligible in comparison with biomarker analyte abundances found in the Devonian rocks (by at least 3 orders of magnitude). Saturate hydrocarbon and aromatic fractions for both sample sets were obtained by silica gel column chromatography; the saturate fractions were eluted with hexane and the aromatic fractions with a 1:1 (v/v) mixture of DCM and hexanes.

### 2.3. MRM-GC-MS

Saturated hydrocarbon fractions were analyzed by metastable reaction monitoring-gas chromatography-mass spectrometry (MRM-GC-MS) conducted at UC Riverside on a Waters Autospec Premier mass spectrometer equipped with an Agilent 7890A gas chromatograph and DB-1MS coated capillary column  $(60 \text{ m} \times 0.25 \text{ mm}, 0.25 \text{ } \mu\text{m} \text{ film}) \text{ using He as carrier gas. The GC}$ temperature program consisted of an initial hold at 60 °C for 2 min, heating to 150 °C at 10 °C/min followed by heating to 320 °C at 3 °C/min and a final hold for 22 min; analyses were performed via splitless injection in electron impact mode, with an ionization energy of 70 eV and an accelerating voltage of 8 kV. MRM transitions for  $C_{27}$ – $C_{35}$  hopanes,  $C_{31}$ – $C_{36}$  methylhopanes,  $C_{21}$ – $C_{22}$ and  $C_{26}$ – $C_{30}$  steranes,  $C_{30}$  methylsteranes and  $C_{19}$ – $C_{26}$  tricyclics were monitored. Procedural blanks with pre-combusted sand yielded less than 0.1 ng of individual hopane and sterane isomers

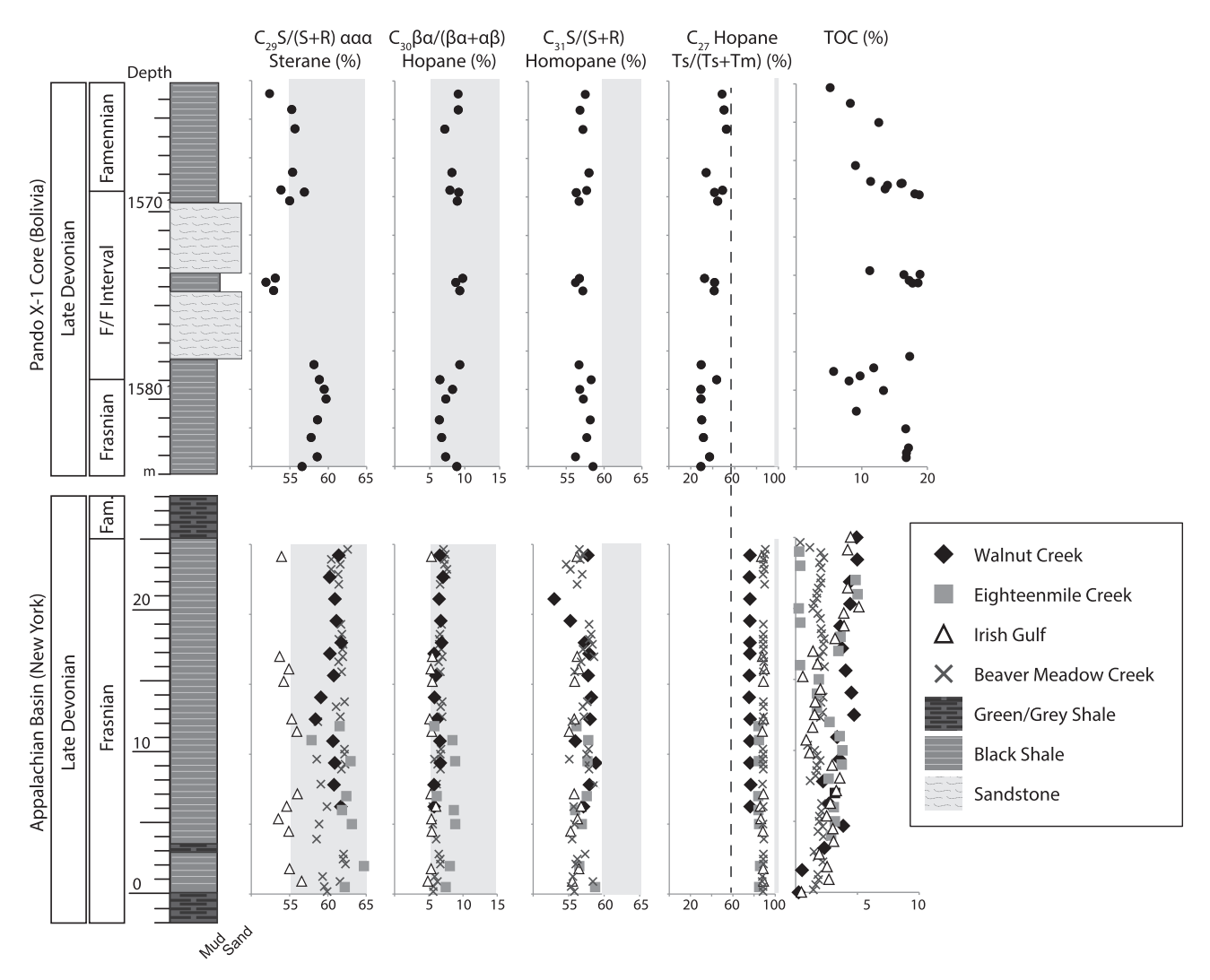


**Fig. 2.** Molecular maturity parameters based on hopane and sterane isomer distributions along with total organic carbon (TOC) content (in weight percent of total rock).  $T_{\text{max}}$  is maximum pyrolysis temperature from Rock-Eval pyrolysis. Shaded bars in molecular parameter plots highlight data points which exceed the theoretical endpoints of thermal equilibration for each parameter (from left to right, 55%, 5%, 60%, 100%; Peters et al., 2005). Dotted line through Ts/(Ts + Tm) plot indicates disparity in maturity between the two basins.

per g of combusted sand. Polycyclic biomarker alkanes (tricyclic terpanes, hopanes, steranes, etc.) were quantified by addition of a deuterated  $C_{29}$  sterane standard  $[d_4\text{-}\alpha\alpha\alpha\text{-}24\text{-ethylcholestane}$  (20R)] to saturated hydrocarbon fractions and comparison of relative peak areas.

### 2.4. GC-MS

The aromatic hydrocarbon fractions were analyzed in both full scan and single ion monitoring methods at UC Riverside by gas chromatography–mass spectrometry (GC–MS) on an Agilent 7890A GC system coupled to an Agilent 5975C inert MSD mass spectrometer. The GC was equipped with a DB1-MS capillary column ( $60 \text{ m} \times 0.32 \text{ mm}$ ,  $0.25 \text{ }\mu\text{m}$  film thickness) and helium was used as the carrier gas. 200 ng of  $d_{14}$ –p-terphenyl standard was added to between 2 and 20 mg of aromatic hydrocarbon fraction for quantification. Chlorobi-derived carotenoid biomarkers, including aryl isoprenoids, isorenieratane, and Palaeozoic and older age selective marker paleorenieratane (Maslen et al., 2009; Melendez et al., 2013b; French et al., 2015) were identified based on m/z 133/134 mass chromatograms, with 2,3,6-trimethyl-substituted aryl isoprenoid abundances measured from m/z 134 ion chromatograms and isorenieratane and paleorenieratane verified from

*m*/*z* 546 molecular ion and retention times (see Fig. 5). Aryl isoprenoid abundances were calculated as TOC-normalized yields; though absolute quantification is not possible without consideration of relative response factors, we are confident our methods allow for internally consistent comparison and accurate crossreference on the scale of order of magnitude with other datasets (Grice et al., 2005; Marynowski and Filipiak, 2007; Marynowski et al., 2007, 2010; Cao et al., 2009) that follow similar methods. To facilitate accurate comparison to other datasets, aryl isoprenoid ratios (AIR) were calculated based on aryl isoprenoid peaks measured from *m*/*z* 133 ion chromatograms, according to the convention set by Schwark and Frimmel (2004).

### 2.5. Elemental and stable isotope analyses

Total organic carbon for the Appalachian Basin samples (Fig. 2) was calculated as the difference between total carbon (TC) and total inorganic carbon (TIC), which were measured using an ELTRA CS 500 carbon–sulfur analyzer equipped with acidification and furnace modules at UC Riverside. Standards AR4012 (limestone, 11.97% carbon) and AR4018 (soil, 1.26% carbon) were used for calibration and average error was ±2% for TC and ±4% for TIC.

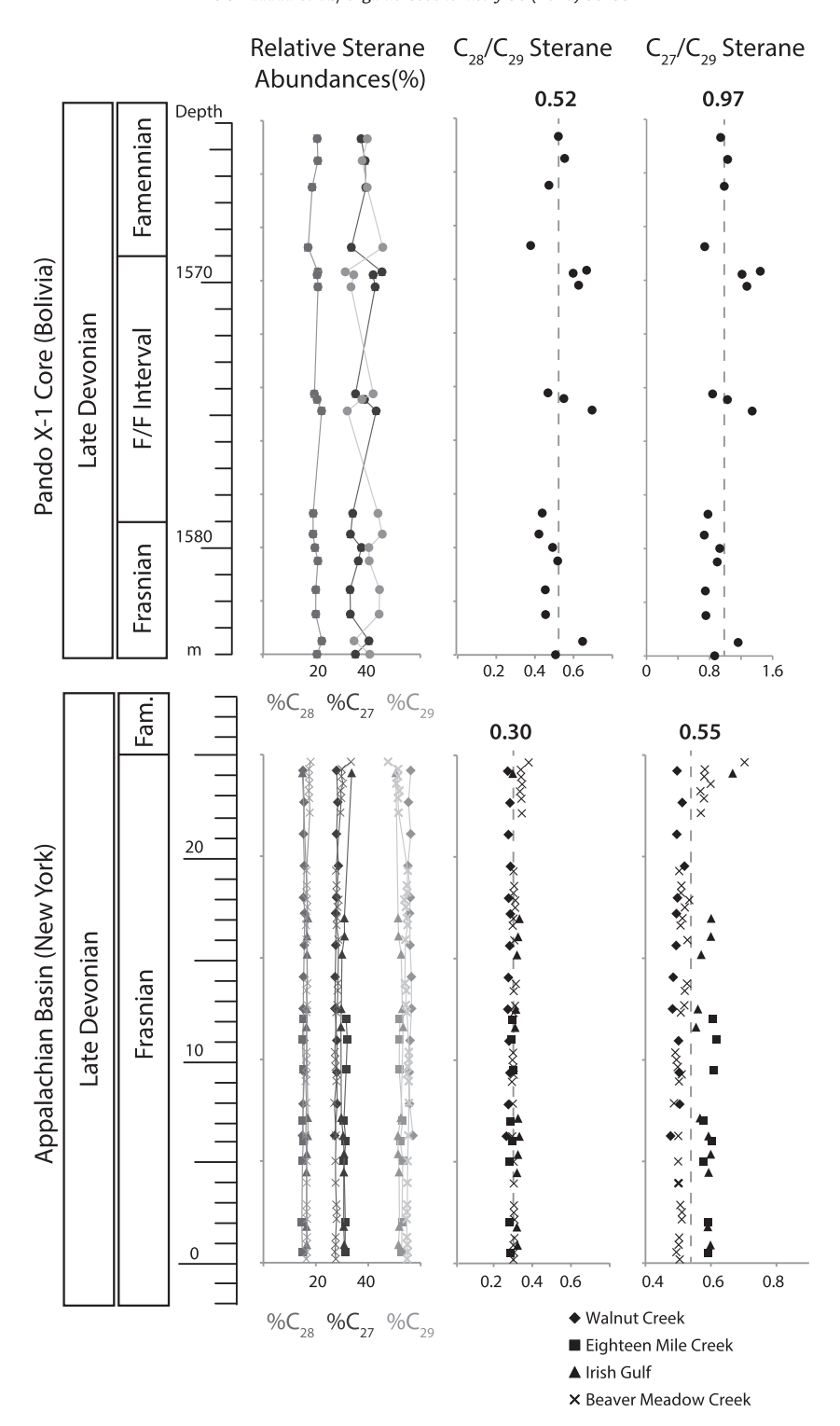
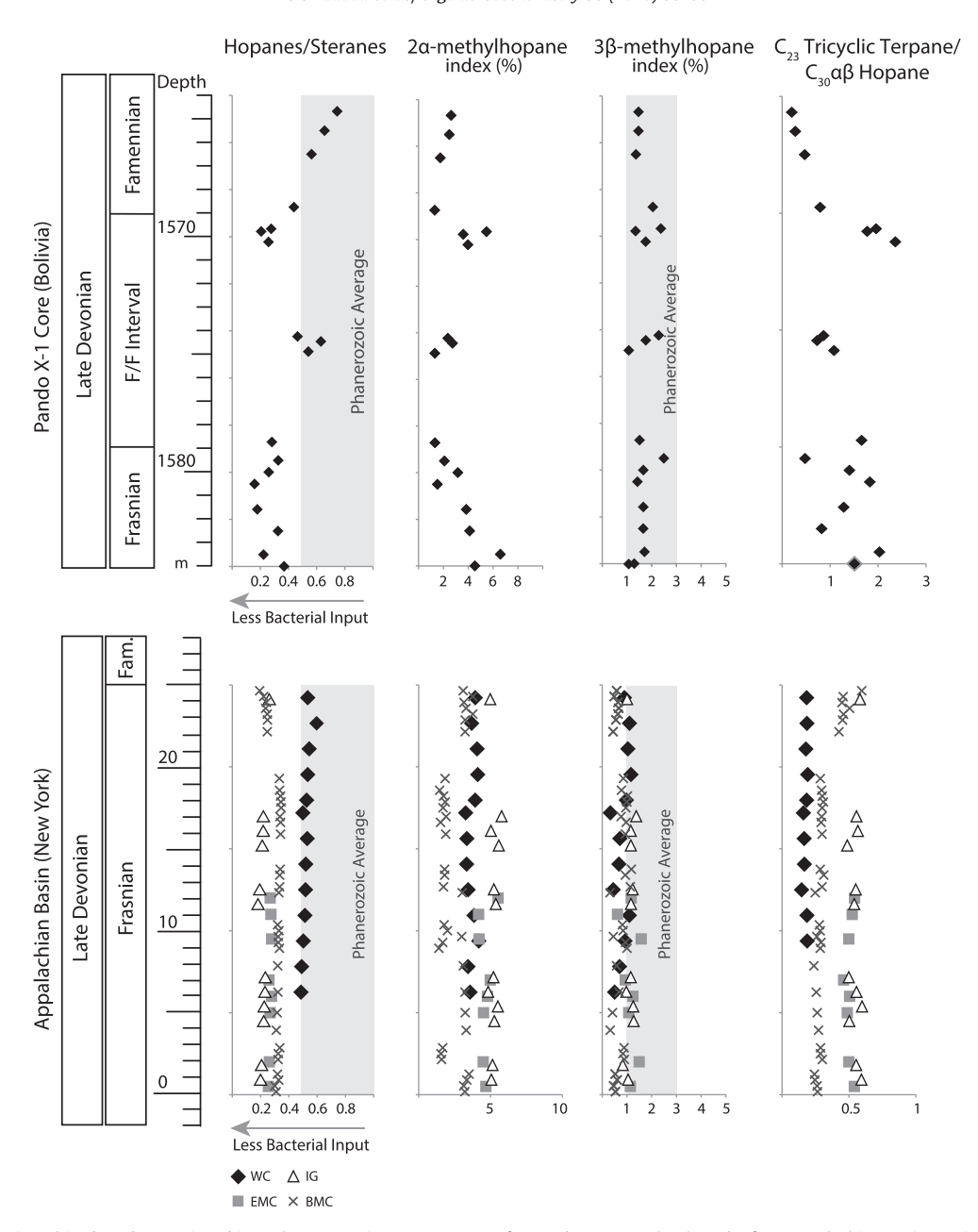


Fig. 3. Sterane carbon number  $(C_{27}-C_{29})$  stratigraphic variations for Pando X-1 core (top) vs the four Appalachian Basin sections (bottom).  $%C_{27}$  steranes =  $C_{27}/(C_{27}+C_{28}+C_{29}+C_{30})$ ;  $%C_{28}$  steranes =  $C_{28}/(C_{27}+C_{28}+C_{29}+C_{30})$ ;  $%C_{29}$  steranes =  $C_{29}/(C_{27}+C_{28}+C_{29}+C_{30})$ . Dotted lines through  $C_{28}/C_{29}$  and  $C_{27}/C_{29}$  plots indicate mean stratigraphic values of the sterane ratios.

Twenty-eight Pando X-1 samples were washed with acetone and ground to <200 mesh size with a ceramic mortar and pestle, acidified with a 30% HCl solution to remove carbonates, washed to neutrality, and dried at 50 °C. The carbonate-free residues were weighed into tin capsules and converted to  $CO_2$  and  $N_2$  for element and isotope analysis using a Costech 4010 elemental analyzer coupled to a Delta V Plus stable isotope ratio mass spectrometer (Thermo Fisher) via a Conflo IV interface (Thermo Fisher). The

mean range of values between duplicate samples for both  ${}^{*}C_{org}$  (TOC) and  ${}^{*}N_{total}$ , (TN) was <2% of the measured abundance. Raw carbon and nitrogen isotope values were corrected using a dual point calibration (Coplen et al., 2006):  $\delta^{13}C_{org}$  values with NBS19 (limestone, 1.95‰) and LSVEC (lithium carbonate, -46.6‰);  $\delta^{15}N_{total}$  values with IAEA-N3 (potassium nitrate, 4.7‰) and USGS34 (potassium nitrate, -1.8‰). The mean range of duplicate samples for  $\delta^{13}C_{org}$  was 0.04‰ and 0.18‰ for  $\delta^{15}N_{total}$ .



**Fig. 4.** Biomarker stratigraphies based on various biomarker source input parameters for Pando X-1 core (top) vs the four Appalachian Basin sections (bottom). Hopanes/steranes =  $C_{27}$ - $C_{35}$  hopanes/ $C_{27}$ - $C_{30}$  steranes. 2α-Methylhopane index (%) = 2α-methylhopane/ $C_{30}$  αβ-hopane; 3β-methylhopane index (%) = 3β-methylhopane/ $C_{30}$  αβ-hopane. Shaded boxes indicate Phanerozoic averages (Peters et al., 2005). WC = Walnut Creek, EMC = Eighteenmile Creek, IG = Irish Gulf, BMC = Beaver Meadow Creek.

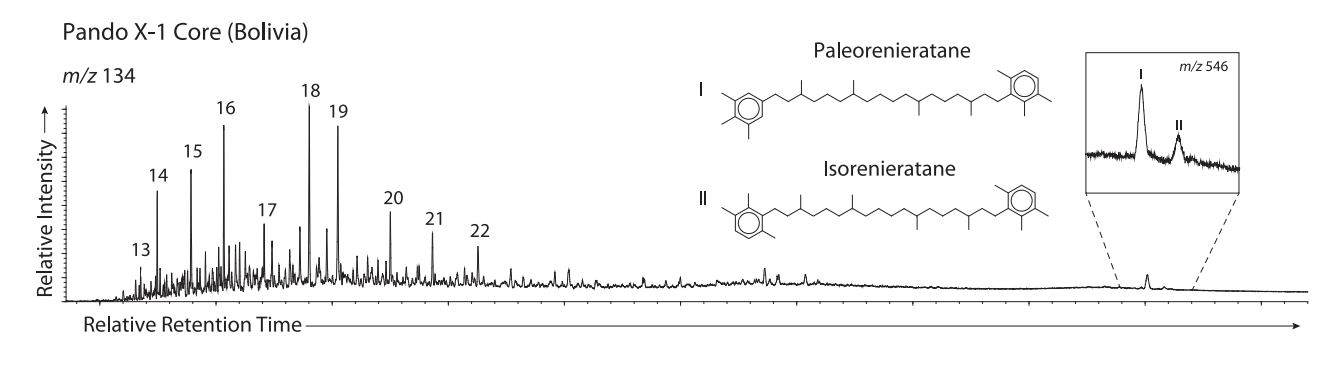
Total phosphorus (TP) was determined using the combustion method (Aspila et al., 1976). Briefly, a 0.5 g aliquot of each sample was combusted at 550 °C for two h, allowed to cool, and shaken overnight in a water bath in a 50 mL 1 N HCl solution at 25 °C. The P content of the decanted solution was determined spectrophotometrically using a molybdate colorimetric reagent. The reproducibility for replicate samples and standards was less than 3.5% of the measured abundance.

## 3. Results and discussion

## 3.1. Thermal maturity parameters

For a total of 18 Madre de Dios samples and the 65 Appalachian Basin samples, abundant rock bitumen extract (12–109 mg of total

bitumen from 5-15 g of rock powder) was generated and a full complement of linear, branched and polycyclic hydrocarbon biomarkers, such as hopanes and steranes and their methylated homologs, was detected using MRM-GC-MS with high signal/ noise ratios. Hopane and sterane maturity ratios are consistent with a mid-oil window stage of thermal maturity (Fig. 2); while most of these alkane biomarker maturity parameters have generally equilibrated, the ratio of C<sub>27</sub> hopane isomers (Ts to Tm; Fig. 2) shows that the Pando X-1 core is less mature than the NY rocks. The disparity in Ts/(Ts + Tm) between the basins is consistent with Rock-Eval parameters, though catalytic effects from clay minerals in the Appalachian Basin may have accentuated the difference (Peters et al., 2005).  $T_{\rm max}$  values for the Pando X-1 core are  $<435\,^{\circ}\text{C}$  (Peters et al., 1997a,b) while Appalachian Basin samples have T<sub>max</sub> values of 440–444 °C and Hydrogen Index (HI) values of 250-380 mg/g TOC, independently verifying that both



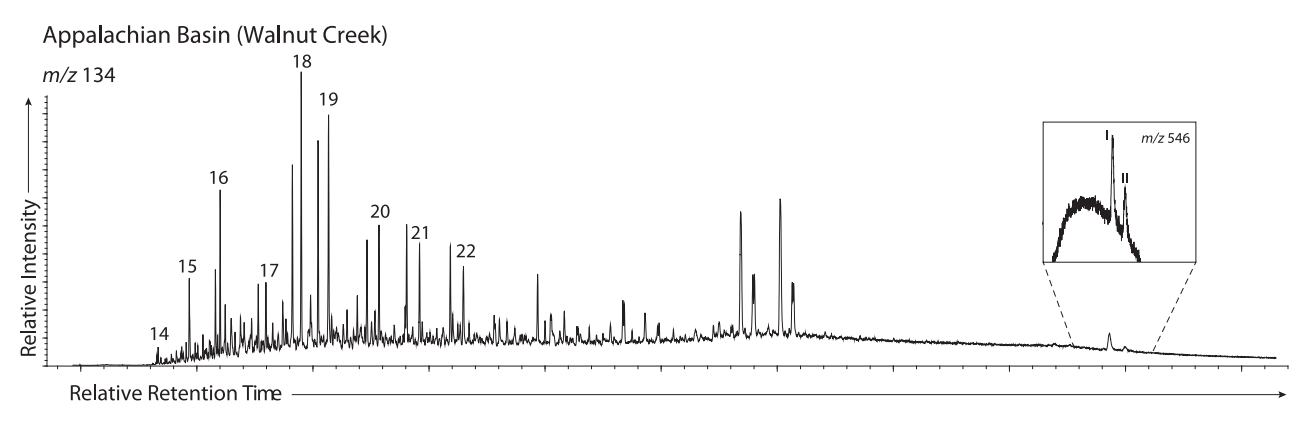


**Fig. 5.** Mass chromatograms (m/z 134) of the Pando 25 (Madre de Dios Basin) and Walnut Creek 80 (Appalachian Basin) samples showing the distribution of paleorenieratane (I), isorenieratane (II), and their aryl isoprenoid derivatives (numbers indicate individual carbon number homologues  $C_{13}$ – $C_{22}$ ). Inset magnifies m/z 546 response of the  $C_{40}$  isoprenoids.

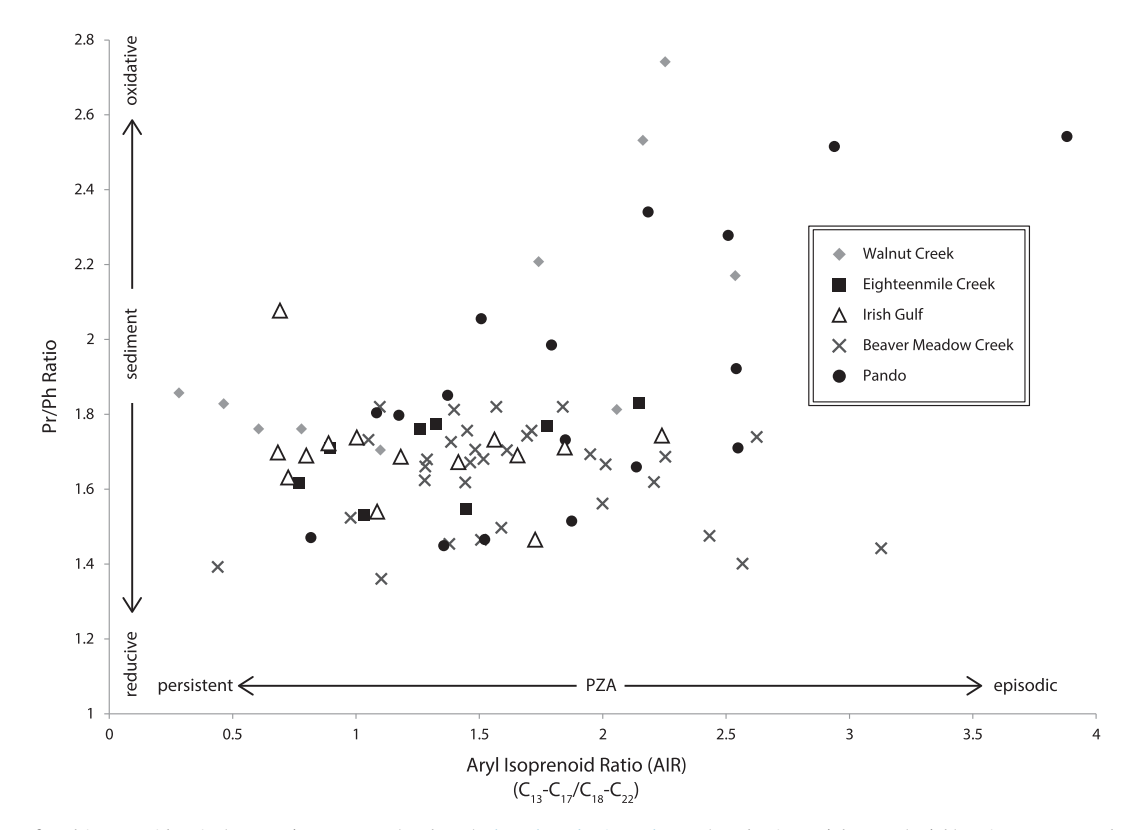


Fig. 6. Cross-plot of aryl isoprenoid ratio ( $C_{13}$ – $C_{17}/C_{18}$ – $C_{22}$ ; AIR) values (Schwark and Frimmel, 2004) and pristane/phytane (Pr/Ph) ratio. Low AIR values indicate more persistent photic zone anoxia (PZA) while higher AIR values indicate episodic PZA. Pr/Ph ratios < 1 are traditionally interpreted as representing deposition under anoxic sediments, though values between 0.8 and 3 should be interpreted with caution due to confounding factors (Peters et al., 2005).

**Table 1**Samples for biomarker analysis, Pando X-1 core, Madre de Dios Basin, Bolivia.

Sample code	Core depth (m)	TOC (wt%)	Bitumen yield (ppt rock)	Saturate fraction	Aromatic fraction					
	• • •		· · · · · · · · · · · · · · · · · · ·	(ppt rock)	(ppt rock)					
	Madre de Dios Basin, Pando X-1 Core									
P1	1564.20	5.61	5.67	0.302	0.552					
P2	1565.02	8.71	5.62	0.562	0.594					
P3	1566.02	13.25	6.74	0.341	0.965					
P4	1568.27	9.53	3.97	0.290	0.508					
P5	1569.10	11.87	n.a.	n.a.	n.a.					
P6	1569.19	16.88	4.74	0.322	0.938					
P7	1569.21	16.93	n.a.	n.a.	n.a.					
P8	1569.30	14.65	5.02	0.403	0.838					
P9	1569.49	14.69	n.a.	n.a.	n.a.					
P10	1569.75	19.00	5.31	0.386	1.04					
P11	1569.80	20.18	n.a.	n.a.	n.a.					
P12	1573.76	11.84	3.78	0.295	0.634					
P13	1573.95	20.19	n.a.	n.a.	n.a.					
P14	1573.97	17.73	5.23	0.441	1.05					
P15	1574.27	17.08	n.a.	n.a.	n.a.					
P16	1574.40	20.11	7.89	0.800	1.61					
P17	1574.41	19.05	n.a.	n.a.	n.a.					
P18	1578.24	18.80	7.99	1.12	1.89					
P19	1578.84	12.22	n.a.	n.a.	n.a.					
P20	1579.02	5.96	3.49	0.620	0.623					
P21	1579.26	10.43	n.a.	n.a.	n.a.					
P22	1579.52	8.92	3.89	0.334	0.794					
P23	1580.02	13.93	5.07	0.570	1.21					
P24	1581.10	9.71	4.48	0.485	0.961					
P25	1582.02	17.34	8.08	0.877	1.61					
P26	1583.02	17.67	5.28	0.400	1.02					
P27	1583.27	17.27	n.a.	n.a.	n.a.					
P28	1583.52	17.66	7.64	0.988	1.49					

ppt rock = Parts per thousand (mg/g) of whole rock powder; n.a. = sample not analyzed for biomarkers but contributed to the elemental and isotope dataset.

these stratigraphic units are ideal for biomarker analysis (Peters et al., 2005). Importantly, both localities reveal diverse and abundant biomarker assemblages.

## 3.2. Microbial ecology from biomarker assemblages

## 3.2.1. Steranes

The steranes in Paleozoic rocks are in general dominated by C<sub>29</sub> steranes (Grantham and Wakefield, 1988; Schwark and Empt, 2006); C<sub>29</sub> steroids are preferentially produced by most green algal clades, which were the major eukaryotic marine phytoplankton in the Paleozoic era (Volkman et al., 1994). In contrast, C<sub>27</sub> and C<sub>28</sub> compounds are most commonly produced as the main steroids by red algae, with C<sub>28</sub> steranes often sourced from more-derived red algal lineages synthesizing chlorophyll a + c that radiated in Mesozoic and younger oceans (dinoflagellates and coccolithophores initially, followed much later in the Cretaceous by diatoms; Huang and Meinschein, 1979; Kodner et al., 2008). Schwark and Empt (2006) found a similar progressive trend through the Phanerozoic as Grantham and Wakefield (1988), but noted C<sub>28</sub>/C<sub>29</sub> sterane ratio excursions at Paleozoic extinction events, specifically the end-Ordovician Hirnantian event, the end-Givetian extinction, the Lower and Upper Kellwasser events, and the Hangenberg extinction event. They identified a persistent shift in sterane compositions after the Hangenberg (Devonian/ Carboniferous boundary) Event, represented by a significant stepwise increase in  $C_{28}/C_{29}$  sterane ratios to values >0.55. An important impetus for this study is the possibility that this pivotal turnover in the phytoplanktonic assemblage may have been triggered by the environmental perturbation associated with the unique accumulation of extinction events in the Late Devonian. The transient spike in  $C_{28}/C_{29}$  which Schwark and Empt (2006) observed at the Frasnian/Famennian boundary event is attributed not to the secular trend toward chlorophyll a + c synthesizing phytoplankton, but instead to an increase in the proportion of prasinophytes to total eukaryotic input, since the Prasinophyceae is the class of green algae which most commonly produces  $C_{28}$  sterols as major sterols (Kodner et al., 2008).

Sterane carbon number patterns (C<sub>27</sub>-C<sub>29</sub>) are surprisingly temporally stable at each location and display no significant stratigraphic variation through either the Pando X-1 core or the 4 different section localities of the Appalachian column (Fig. 3), with the greatest differences in biomarker assemblages observed between the two different marine settings (Pando vs Appalachian). Notable though is the distinct offset in both the  $C_{27}/C_{29}$  and  $C_{28}/C_{29}$ sterane ratios between the two basins, attributable mainly to a much lower contribution from  $C_{29}$  sterol-synthesizing algae in the Madre de Dios Basin than the Appalachian Basin. Both  $C_{27}/C_{29}$  and  $C_{28}/C_{29}$  sterane ratios remain consistently high through the Frasnian, F/F and Famennian intervals of the Pando X-1 core,  $(C_{27}/C_{29} \text{ min} = 0.73, \text{ max} = 1.44, \text{ mean} = 0.98; C_{28}/C_{29} \text{ min} = 0.38,$ max = 0.70, and mean = 0.53), but are significantly lower in each of the Appalachian Basin localities  $(C_{27}/C_{29})$  min = 0.48, max = 0.70, mean = 0.55;  $C_{28}/C_{29}$  min = 0.16, max = 0.38,mean = 0.30). Additionally, strong  $C_{30}$  sterane signals, in the form of 24-n-propylcholestane isomers likely sourced from pelagophyte algae (Volkman, 2003; Rohrssen et al., 2015), were detected throughout both the Pando X-1 core and Appalachian Basin sample sets. This sterane pattern is in stark contrast to other earlier Paleozoic marine rocks from the Cambrian to Early Silurian for which 24-n-propylcholestane is often not detectable even using MRM-GC-MS (Rohrssen et al., 2015).

The mean proportional abundances of  $C_{27}$ ,  $C_{28}$ , and  $C_{29}$  steranes between the Appalachian Basin and the Pando X-1 core are statistically distinct ( $p \ll 0.05$ ), indicating that the large differences in both the  $C_{27}/C_{29}$  and  $C_{28}/C_{29}$  ratios are not controlled just by a change in input from  $C_{29}$  sterols. Rather, it is clear that there is increased eukaryotic contribution in the Madre de Dios Basin from both red algal lineages ( $C_{27}$  sterol producers) and  $C_{28}$  sterol producing green algae (likely Prasinophyceae; Kodner et al., 2008) concomitant to a proportional decrease in  $C_{29}$  sterol-producing green algae (probably Chlorophyceae; Kodner et al., 2008), while the Appalachian Basin samples display much more traditionally Paleozoic signals of  $C_{29}$  sterol dominance.

The  $C_{28}/C_{29}$  sterane ratios for the Pando X-1 core are consistent with Schwark and Empt's (2006) general findings: a maximum C<sub>28</sub>/C<sub>29</sub> value of 0.70 in the F/F interval indicates increased contribution from C<sub>28</sub> sterol synthesizing algae during the deposition of this Upper Kellwasser equivalent black shale. An interpretation favoring increased prasinophyte input as an explanation for the C<sub>28</sub> sterane abundance is consistent with an apparent prasinophyte-dominated palynology of the Pando X-1 core samples which show abundant Tasmanites cysts (de la Rue, 2010). Palynological support for an algal assemblage with rich contributions from prasinophytes is lacking in the low-latitude Appalachian Basin, an observation consistent with both the tricyclics/hopanes ratios and the sterane ratios we measured there (see Section 3.2.4). Appalachian Basin samples display normal Paleozoic sterane signals lacking the anonymously inflated  $C_{28}/C_{29}$  ratios we see in the Pando X-1 core. This latitudinal difference in primary producer ecology is not unexpected, as Tasmanites and other prasinophyte algae have a well known association with high-latitude marginal marine settings, like that of the Madre de Dios Basin (Revill et al., 1994; Peters et al., 2005).

## 3.2.2. Hopane/sterane relationship

Hopane  $(C_{27}-C_{35})$ /sterane  $(C_{27}-C_{30})$  ratios (H/S) in the Pando X-1 core show a statistically significant (p < 0.05) difference

**Table 2**Samples for biomarker analysis, Appalachian Basin, New York, USA, from most shoreward to most proximal: Beaver Meadow Creek, Irish Gulf, Eighteenmile Creek, Walnut Creek.

Ritumen Sample code Strat. TOC Saturate Aromatic depth (wt%) vield fraction fraction (ppt rock) (ppt rock) (ppt rock) (cm) Beaver Meadow Creek BMC 0.5 68.5 1.44 3.31 1.49 0.81 **BMC 15** 1.63 1 37 0.89 67.5 3 4 7 BMC 2.5 66.5 1.86 3.94 1.83 1.03 BMC 3.5 65.5 3.79 1.02 1.80 1.72 BMC 6 63 2.21 4.18 1.62 1.26 0.84 BMC 7 62 3.02 1.02 174 BMC 8 61 1.50 3.04 0.90 0.90 BMC 11 58 2.25 4.96 1.86 1.56 BMC 12 57 1.81 3.80 1.44 0.64 **BMC 13** 56 5.21 1.32 0.99 2.19 **BMC 14** 55 1 91 473 183 1 54 **BMC 15** 54 1.94 4.43 1.37 0.88 BMC 16 53 2.09 4 23 1.42 0.89 BMC 17.5 51.5 8.87 1.60 2.13 2.11 **BMC 22** 47 1 18 2 30 0.60 0.72 BMC 23 4.09 1.08 0.90 46 1.62 **BMC 24** 45 1.71 4.36 1.53 1.08 **BMC 25** 1.26 0.81 44 1.73 4.18 **BMC 26** 43 1.60 1 30 1 99 4 5 2 **BMC 27** 42 1.73 3.93 1.68 1.60 **BMC 28** 1.54 3.78 1.20 1.12 BMC 29 40 0.97 2.30 0.55 0.70 RMC 34 5 345 2.02 453 1.62 1 35 BMC 35.5 33.5 2.19 4.18 1.35 1.08 BMC 37.5 31.5 2.05 4.26 1.35 1.17 BMC 38.5 30.5 2.23 4.54 1.50 1.00 **BMC 44 5** 245 2.34 4 48 1 53 1 26 BMC 46.5 22.5 1.96 4.22 1.26 0.99 BMC 47.5 21.5 2.22 4.24 1.35 1.35 BMC 49 20 2.25 4.64 1.20 1.00 BMC 50 19 2.32 4.84 1.50 1.00 BMC 51 18 2.11 5 34 1 32 1 32 BMC 52 17 2.07 4.26 1.35 1.35 BMC 54 15 2.01 3 62 1.20 1 20 BMC 55 3.40 0.84 14 1.80 1.19 BMC 56 13 1 39 3 48 0.98 N 98 **BMC 57** 0.98 0.70 12 1.48 3.42 **BMC 58** 11 1.71 3.18 0.96 0.60 BMC 59 0.80 10 1.72 4.06 1.28 BMC 60 g 1.05 1.84 3 44 112 **BMC 61** 8 2.06 2.96 0.72 0.66 BMC 62 2.02 2.80 1.02 1.02 **BMC 64** 5 2.07 2.94 1.08 1.08 **BMC 65** 4 1 94 3 10 0.84 1.05 **BMC 66** 3 2.29 3.04 1.05 0.91 2 2.98 0.90 **BMC 67** 2.05 1.08 **BMC 68** 1.15 2.02 0.60 0.64 BMC 69 O 0.830 0.26 0.34 0.37 Irish Gulf IG 108 1 4 22 4 12 1 09 1 09 IG 116 9 1.41 4.13 1.50 0.95 IG 117 10 4.40 1.35 1.03 1.77 IG 118 11 0.59 3.75 1.43 1.03 IG 121 1.54 2.87 0.89 14 1.13 0.52 IG 122 15 138 193 0.68 IG 127 20 3.29 5.09 2.09 1.49 IG 128 21 2.82 4.57 1.86 1.47 IG 129 22 2.51 4.33 2.31 1.44 IG 130 23 3.01 4 08 175 1.43 IG 131 24 3.07 3.74 1.32 1.01 26 IG 133 2.55 4.38 1.85 1.06 IG 134 2.70 1.74 1.03 4.21 Eighteenmile Creek EMC 0.5 245 2.60 5 34 1 20 0.48 EMC 2 2.87 4.22 1.24 1.33 23 EMC 5 20 3 18 3 3 5 0.62 1 25 EMC 6 19 3.09 4.61 0.89 1.19 EMC 7 18 3.19 3.11 1.40 1.19

Table 2 (continued)

Sample code	Strat. depth (cm)	TOC (wt%)	Bitumen yield (ppt rock)	Saturate fraction (ppt rock)	Aromatic fraction (ppt rock)	
EMC 9.5	15.5	3.74	3.93	1.60	1.20	
EMC 11	14	3.57	4.57	1.28	1.48	
EMC 12	13	2.74	4.55	1.18	2.07	
EMC 17	8	3.46	0.80	0.10	0.16	
EMC 18	7	3.64	0.91	0.12	0.10	
EMC 23	2	0.37	0.69	0.12	0.08	
Walnut Creek	Walnut Creek					
WC 74.5	0	5.53	4.00	0.88	0.88	
WC 75.5	1	4.94	5.34	1.43	1.98	
WC 76.5	2	4.99	5.70	1.20	1.80	
WC 77.5	3	4.40	4.68	1.30	1.40	
WC 78.5	4	4.42	4.76	1.30	1.40	
WC 79.5	5	3.62	4.64	1.40	1.40	
WC 80	5.5	3.77	4.86	1.59	1.69	
WC 81	6.5	4.05	5.53	1.65	1.65	
WC 82	7.5	4.51	5.24	1.40	1.50	
WC 83	8.5	4.73	4.25	1.20	1.60	
WC 84	9.5	3.36	4.36	1.17	1.26	
WC 85	10.5	3.55	4.38	1.26	1.53	
WC 86	11.5	2.22	3.92	1.20	1.12	
WC 87	12.5	2.70	4.09	1.60	1.60	
WC 93	18.5	2.64	4.75	1.98	1.78	

Strat. depth = stratigraphic depth where top of Upper Kellwasser black shale = 0 cm; ppt rock = parts per thousand (mg/g) of whole rock powder.

between the mean ratio in the Frasnian interval (0.27) and those in the F/F (0.55) and Famennian (0.45) intervals, reflecting both an excursion in the F/F section toward slightly higher H/S values and a trend toward higher values in the youngest core samples, notably a return to H/S values within the Phanerozoic average of 0.5–2.0 for ancient source rocks (Peters et al., 2005) in the early Famennian. All measured H/S values, however, are low, with the composite average of 0.38 (min = 0.16, max = 0.75) falling below this Phanerozoic average, indicating eukaryotic-rich organic inputs. The H/S values in the Appalachian Basin localities are similarly and characteristically low, with the three most shoreward localities having a mean H/S of 0.27; Walnut Creek, the most distal locality, displays distinct H/S values (mean = 0.53) and the majority of samples analyzed from this locality fall within the range of Phanerozoic marine averages (Peters et al., 2005) (Fig. 4).

The abnormally low H/S reported here from the Pando X-1 core and the Appalachian Basin localities indicate high relative input of eukaryotes during deposition of the Upper Kellwasser equivalent sediments in both high- and low-latitude basins, despite apparent persistent N limitation (based on C/N/P relationships, see Section 3.4.1.) that might be expected to have favored prokaryotic diazotrophs. These ratios contrast with extremely elevated H/S in nitrogen-limited epeiric settings during other Phanerozoic extinction events, including the Late Ordovician (Rohrssen et al. (2013) report a Hirnantian excursion of H/S in excess of 12) and the earliest Triassic aftermath of the Permo-Triassic Mass Extinction (Cao et al., 2009 report H/S up to 60 following the extinction boundary in Meishan, China); these characteristically high H/S values may point to bacterially-dominated assemblages and algal-production limited by denitrification (LaPorte et al., 2009). The low H/S values reported here for the Upper Kellwasser, however, are consistent with high algal production that was sustained by efficient remineralization of organic N and P in the water column and underlying sediments and a relatively small contribution to overall biomass from diazotrophs, consistent with the model of Higgins et al. (2012) for primary production during Cretaceous OAEs.

#### 3.2.3. Methylhopanes

Methylhopane ratios similarly suggest no strong excursions through the Upper Kellwasser interval in either basin, although in the Pando X-1 core they show slight variation between the three lithologic packages (Fig. 4). 3β-Methylhopanes are derived from 3β-methylbacteriohopanepolyols synthesized by both aerobic methanotrophic proteobacteria and acetic acid bacteria (though methanotrophs are the likely dominant contributor to marine source rocks at circum-neutral seawater pH; Farrimond et al., 2004); elevated 3β-methylhopane index (3-MeHI) values in marine rocks are therefore thought to reflect significant environmental methane cycling (Rohrssen et al., 2015). In the Madre de Dios samples, 3-MeHI values do not systematically vary from the mean of 1.7% (min = 1.1%, max = 2.5%), and all values are within the range of Phanerozoic averages for typical marine petroleum source rocks (1–3%; Farrimond et al., 2004; Cao et al., 2009). In the Appalachian samples, 3-MeHI values average 1.0% (min = 0.3%; max = 1.6%). Values are generally lower for both Beaver Meadow Creek (mean = 0.8; min = 0.3%; max = 1.2%) and Walnut (mean = 0.8; min = 0.3%; max = 0.7%), but are not exceptional for Phanerozoic assemblages. Indeed, what is exceptional is the Upper Kellwasser shale's divergence in 3-MeHI values from other significant Phanerozoic extinction events: notably, elevated 3-MeHI values have been measured from both Late Ordovician (3-MeHI in the range 1.7-12%; Rohrssen et al., 2013) and Late Permian-Early Triassic bitumens (3-MeHI in the range 1.6-7%; Cao et al., 2009), but anomalously high values are not observed in either Late Devonian basin studied here.

The 2α-methylhopane index (2-MeHI) was previously used to constrain cyanobacterial input to sedimentary organic matter (Summons et al., 1999); although more recent research has shown that  $2\alpha$ -methylhopanes are not necessarily sourced solely by cyanobacteria or indicative of oxygenic photosynthesis when they are (Rashby et al., 2007; Doughty et al., 2009; Welander et al., 2010). Elevated 2-MeHI values have been reported during and in the aftermath of other Phanerozoic oceanic anoxic events (Kuypers et al., 2004: Dumitrescu and Brassell, 2005), sometimes contemporaneous to shifts in N isotopic signatures implying nitrate limitation (Kuypers et al., 2004). As such, we monitored 2-MeHI in our sections as stratigraphic trends. 2-MeHI values in the Pando X-1 core are low through the F/F interval (mean: 2.1%), and comparatively slightly elevated through the Frasnian (mean: 3.4%) and Famennian (mean: 3.0%) intervals; 2-MeHI values for the Appalachian Basin samples are uniformly higher, with a basinal mean of 4.1%, with the most proximal locality, Beaver Meadow Creek, displaying the lowest values (min = 1.4%, max = 3.8%, mean = 2.3%; Fig. 4), then the most distal locality, Walnut Creek (min = 3.3%, max = 4.2%, mean = 3.7%), then Eighteen Mile Creek (min = 4.2%, max = 5.5%, mean = 4.7%), and Irish Gulf (min = 4.8%, max = 5.8%, mean = 5.3%), following no clear basinal trend.

All 2-MeHI values for the Upper Kellwasser sediments are comparably low and not indicative of unusually high input from 2-methylbacteriohopanepolyol-synthesizing bacteria to either the Appalachian or Madre de Dios Upper Kellwasser organic matter. While this is to our knowledge the first reported 2-MeHI data for Upper Kellwasser-equivalent sediments, Marynowski et al. (2011) reported consistently elevated 2-MeHI values (6.1–13.4%) in early Famennian strata overlying the Upper Kellwasser depositional event at Kowala, Poland. These biomarkers, coupled with microstratigraphic data for cyanobacterial mats, are cited as evidence for increased opportunistic microbial activity following environmental perturbation associated with mass extinction. Lack of elevated 2-MeHI values in the Upper Kellwasser black shales also contrasts with elevated 2-MeHI values from Cretaceous organic-rich depositional events, specifically the early Aptian

ocean anoxic event OAE 1a and late Cenomanian OAE 2. Kuypers et al. (2004) report 2-MeHI values up to 20% for both events; Dumitrescu and Brassell (2005) report 2-MeHI values up to 39% for OAE 1a and 45% for OAE 2.

#### 3.2.4. Tricyclic terpanes

Tricyclic terpanes have been proposed previously to be biomarkers diagnostic of *Tasmanites*, a prasinophycean algal genus, due to their consistent occurrence and abundance in Tasmanite oil shales, like that of the Tomachi Formation (Simoneit and Leif, 1990; Aquino Neto et al., 1992; Greenwood et al., 2000). The biological affinity of these molecules, however, has been called into question (Dutta et al., 2006) as *Leiosphaeridia* palynomorphs were found to be another likely source organism of the compounds and, more generally, due to the ubiquity of tricyclic terpanes in ancient rocks and oils. Furthermore, elevated tricyclic terpanes/hopane ratios are found at high thermal maturity (due to the higher stability of tricyclic terpanes) and in saline depositional settings (organic facies control) (Peters et al., 2005).

Due to extensive microfossil evidence in the Tomachi Formation from the same Pando X-1 core for an abundance of tricyclic terpane-associated palynomorphs, including Tasmanites, Leiosphaeridia and other prasinophytes (de la Rue, 2010), we examined the trends of  $C_{23}$  tricyclic terpane/ $C_{30}$  17 $\alpha$ ,21 $\beta$ -hopane in both basins: the average tricyclics/hopane ratio in the Pando X-1 core is 1.20 (range = 0.20-2.36), while the composite average tricyclics/hopanes ratio from the four Appalachian Basin localities is lower at 0.39 (range = 0.15-0.60; Walnut Creek mean = 0.17; Eighteenmile Creek mean = 0.51; Irish Gulf mean = 0.55; Beaver Meadow Creek mean = 0.32; Fig. 4). While the Appalachian Basin samples were not tested directly for microfossils like the Pando X-1 samples, at least one study (Schieber and Baird, 2001) reports pyrite spheres that are interpreted as Tasmanites cysts from the same New York strata; while the relative abundance of tricyclic terpane-related palynomorphs in the Appalachian Basin samples is unknown, Schieber and Baird (2001) anecdotally note that Tasmanites appear more common in Famennian mudstones than in the late Frasnian Upper Kellwasser shales. While the Pando X-1 core samples do exhibit higher values of tricyclics/hopanes, the relatively small difference in mean values versus the Appalachian samples and significant range of ratio values found do not necessarily support a single origin of tricyclic terpanes from Tasmanites, despite the very high abundance of these fossil cysts in the Pando X-1 core.

## 3.3. Marine paleoredox indicators

## 3.3.1. Chlorobi markers

The aromatic carotenoid pigment molecule produced by green sulfur bacteria Chlorobi, isorenieratene, can be well-preserved in sediments of low thermal maturity as the molecular fossil isorenieratane and its diagenetic fragments, aryl isoprenoids (Summons and Powell, 1986). These molecules indicate that free hydrogen sulfide was present at least episodically up into the photic zone of the water column (Summons and Powell, 1987) during deposition of these strata because Chlorobi are strictly anaerobic, obligate phototrophs using mainly H<sub>2</sub>S as an electron donor for photosynthesis. As such, isorenieratane and aryl isoprenoids are considered robust markers for recognizing periods of photic zone euxinia (PZE).

Previous biomarker studies in the Late Devonian have found evidence for photic zone euxinia in different epeiric basins at sub-tropical to tropical latitudes (in Europe, western Canada, Australia, and North America; Summons and Powell, 1986; Hartgers et al., 1994; Clifford et al., 1998; Joachimski et al., 2001; Brown and Kenig, 2004; Melendez et al., 2013a). Joachimski et al.

(2001) and Marynowski et al. (2011) found Chlorobi biomarkers in all samples across the Frasnian/Famennian boundary and into the early Famennian in the Kowala quarry of the Holy Cross Mountains, Poland, including isorenieratane and a series of  $C_{13}$ – $C_{22}$  aryl isoprenoids with a 2,3,6-trimethyl substitution pattern on the aromatic ring (Summons and Powell, 1986). Brown and Kenig (2004) expanded the scope of Devonian biomarker investigations of low-latitude epeiric seas to the Laurentian Michigan and Illinois Basins and reported aromatic carotenoid biomarkers for green sulfur bacteria in Middle Devonian–Early Mississippian black and green/gray shale, despite explicit indications of sedimentary bioturbation in the latter samples.

Isorenieratane and paleorenieratane were detected only in trace amounts in eight samples from the Pando X-1 core (20-25 and 1-3) in the Frasnian and Famennian intervals; no isorenieratane was detectable in the F/F interval. The C<sub>40</sub> compounds were also detected in three of the Appalachian Basin localities (not at Eighteenmile Creek), but just above detection limits, in even lower amounts than in the Pando X-1 core. Both isorenieratane and paleorenieratane were detected in Walnut Creek samples (see Fig. 5); only paleorenieratane was present in high enough abundances to be detected in Irish Gulf and Beaver Meadow Creek samples. Aryl isoprenoid abundances for the Pando X-1 core range from 0.92-6.57 ppm TOC (Table 3), displaying no significant variation through the core or between the three intervals; aryl isoprenoid abundances for the Appalachian Basin localities range from 0.08-16.3 ppm TOC across the four localities, with the highest abundances occurring in sediments from the most distal, Walnut Creek, and the most shoreward, Beaver Meadow Creek, localities (Table 3). All the summed absolute abundances of 2,3,6-trimethyl-substituted aryl isoprenoids and C<sub>40</sub> aromatic carotenoids measured though were very low in magnitude.

While the presence of detectable aryl isoprenoids and trace quantities of isorenieratane and paleorenieratane provide evidence for at least intermittent photic zone euxinia in the Madre de Dios Basin during the deposition of the Tomachi Formation and in the Appalachian Basin during the deposition of the Hanover Formation (and specifically the Point Gratiot Bed), a simple presence vs absence binary indication from these compounds alone is not as informative for understanding dynamic water column chemistry as a more quantitative consideration of the absolute abundance of green sulfur bacteria markers and their relative contribution to sedimentary organic matter. Both Pando X-1 core samples and Appalachian Basin samples contain very low amounts of  $C_{13}$ – $C_{22}$ aryl isoprenoids, in similar concentrations (mean: 3.5 ppm TOC for the Pando X-1 core; mean: 6.7 ppm TOC for the Appalachian Basin; see Table 3) as those reported from the middle Famennian of Poland (C<sub>13</sub>-C<sub>22</sub>, mean: 3.7 ppm TOC; Marynowski et al., 2007); these low concentrations in the Holy Cross Mountains of Poland were attributed to only episodic photic zone euxinia, in contrast to persistence of a sulfidic chemocline into the photic zone, and the concentrations in the Pando X-1 core and Appalachian Basin are interpreted similarly.

Importantly, though, the aryl isoprenoid concentrations reported here are much lower than concentrations reported at

other black shale events in the Late Devonian, including during the Famennian Dasberg event ( $C_{13}$ – $C_{22}$ , max: 143.5 ppm TOC; Marynowski et al., 2010) and the end-Famennian Hangenberg event (C<sub>13</sub>-C<sub>22</sub>, max: 120 ppm TOC; Marynowski and Filipiak, 2007), both as expressed in the Holy Cross Mountains of Poland. These Devonian events, in turn, track aryl isoprenoid abundances up to an order of magnitude lower than concentrations reported from other euxinic basins through the Phanerozoic, especially during the Permo-Triassic (P-T) mass extinction for rocks of similar thermal maturity. At the Meishan section in southern China, Cao et al. (2009) measured C<sub>14</sub>-C<sub>27</sub> aryl isoprenoid abundances of 2723 ppm TOC during the Changhsingian leading into the P-T mass extinction event and 2301 ppm TOC at the P-T boundary. While most research supports that PZE was widespread during the P-T extinction, it has been observed that local redox and nutrient variations impact green sulfur bacteria production: Grice et al. (2005) reported individual aryl isoprenoid abundances (C18, C19 and C<sub>20</sub>) at the P-T boundary from the Perth Basin, Western Australia, with single aryl isoprenoid compound values up to 90 ppm TOC though with isorenieratane abundances reaching less than 30 ppm TOC, but implying summed yields generally in the  $10^2$ – 10<sup>3</sup> ppm range.

#### 3.3.2. AIR values and pristane/phytane ratios

To further test whether these low aryl isoprenoid abundances might be attributable to episodic photic zone euxinia, we employed the aryl isoprenoid ratio (AIR), which uses the proportion of short-chain  $(C_{13}-C_{17})$  to intermediate-chain  $(C_{18}-C_{22})$  aryl isoprenoids to assess the degree to which these compounds underwent aerobic degradation during episodic oxygenation events between periods of photic zone euxinia (Schwark and Frimmel, 2004). Higher AIR values (or a greater relative proportion of short-chain aryl isoprenoids) are indicative of shorter and more punctuated periods of anoxia pervading into the photic zone, while lower AIR values indicate more persistent and intensive photic zone euxinia. AIR values for the four Appalachian Basin localities and the Pando X-1 core range between 0.27-3.88 (Fig. 6); each of the localities fluctuates between lower values indicative of persistent photic zone anoxia and high values indicative of episodic photic zone anoxia, or oxygenation events (Walnut Creek: min = 0.27. max = 2.54,mean = 1.40; Eighteenmile Creek: min = 0.77, max = 2.15, mean = 1.33; Irish Gulf: min = 0.69, max = 2.24, mean = 1.25; Beaver Meadow Creek: min = 0.44, max = 3.13, mean = 1.65: Pando X-1 core: min = 0.82, max = 3.88, mean = 1.95). In contrast to Schwark and Frimmel's (2004) dataset, however, the concentration of aryl isoprenoids does not negatively correlate with the AIR values; rather, there is no correlation and, in fact, the Pando X-1 core samples and Appalachian Basin Eighteenmile Creek and Beaver Meadow Creek samples display weakly positive correlations between aryl isoprenoid abundance and AIR values.

Plotting the AIR against pristane/phytane ratios helps to identify the extent of redox control (vs a possible maturity control or other factor) on the ratio of short-chain to intermediate-chain aryl isoprenoids. Pristane/phytane (Pr/Ph) ratios are weakly specific for redox conditions because reducing conditions promote the

 Table 3

 Ranges and means of aryl isoprenoid (A.I.  $C_{13}$ – $C_{22}$ ) and summed isorenieratane and paleorenieratane (Iso./Paleo.) abundances for each locality.

Locality	A.I. C <sub>13</sub> -C <sub>22</sub> range (ppm TOC)	A.I. C <sub>13</sub> -C <sub>22</sub> mean (ppm TOC)	n=	Iso./Paleo. range (ppm TOC)	Iso./Paleo. mean (ppm TOC)
Beaver Meadow Creek	1.44-16.3	9.04	44	0.12-0.72	0.26
Irish Gulf	0.67-12.3	3.37	14	0.06-0.61	0.17
Eighteenmile Creek	0.08-4.60	2.37	11	n.d.	n.d.
Walnut Creek	7.81–15.8	10.98	10	0.07-0.73	0.30
Pando X-1 Core	0.92-6.57	3.50	18	0.06-0.61	0.13

conversion of the phytyl side chain of chlorophyll to phytane, while oxic conditions favor the conversion of phytyl to pristane (Peters et al., 2005). Accordingly, higher Pr/Ph ratios suggest oxic depositional conditions, with lower ratios suggesting reducing depositional conditions. Multiple confounding factors, however, contribute to the limited utility of this biomarker (Koopmans et al., 1999; Peters et al., 2005), though very low values (<0.8) probably indicate anoxic, possibly hypersaline environments, and very high values (>3.0) most likely indicate terrigenous input under oxic conditions. Pr/Ph ratios for the Appalachian Basin (Walnut Creek: min = 1.70, max = 2.74, mean = 2.04; Eighteenmile Creek: min = 1.53, max = 1.83, mean = 1.69; Irish Gulf: min = 1.46, max = 2.08, mean = 1.70; Beaver Meadow Creek: min = 1.35, max = 1.83, mean = 1.62) and Pando X-1 core (min = 1.39, max = 2.52, mean = 1.86) are uniformly high (Fig. 6), consistent with depositional environments that are not highly reducing. Notably, the Pando X-1 core samples and the most distal Appalachian Basin locality, Walnut Creek, display a positive correlation between the Pr/Ph ratios and AIR values, suggesting that the AIR values in these samples are indeed redox controlled. This lends greater support to a direct interpretation of the higher AIR values reflecting episodic photic zone euxinia in the Madre de Dios Basin and the deep Appalachian Basin (Walnut Creek), as suggested by the low absolute abundances of aryl isoprenoids. Because samples from Eighteenmile Creek Irish Gulf, and Beaver Meadow Creek do not display clear covariance between AIR and Pr/Ph ratios or AIR and aryl isoprenoid abundances, it is not clear whether a redox control on AIR can be reasonably inferred for these samples. Further paleoenvironmental multiproxy work will serve to clarify the significance of the redox-sensitive biomarkers detected in Frasnian/ Famennian sediments and the marine redox chemistry of both the Appalachian and Madre de Dios Basins.

## 3.4. Carbon, nitrogen, and phosphorus

## 3.4.1. Elemental C/N/P

Total organic carbon (TOC) content of the Madre de Dios samples ranges from 5–19%, with an average TOC of 13.8%; TOC for the Appalachian samples is much lower, with a range of 0.5–5% and the mean TOC for each locality decreasing shoreward (Walnut Creek = 3.1%; Eighteenmile Creek = 2.5%; Irish Gulf = 2.3%; Beaver

Meadow Creek = 1.8%; Fig. 2). Because TOC and TN are characteristically well correlated, the molar ratio of organic C to organic N (ON), determined by the slope of a regression of TN and TOC (Calvert, 2004), for the Pando X-1 samples is 44.5 (Fig. 7A). The positive intercept on the TN axis indicates that a consistent 0.084% of each sample is inorganic N, possibly in the form of ammonium bound in clay mineral matrices (Müller, 1977; Calvert, 2004). For the increasingly distal intervals at Perry Farm, Irish Gulf, and Walnut Creek the values of TOC/ON rise systematically from 38.5 to 46.1 to 51.8 (Tuite and Macko, 2013). Similarly, the mean of the ratio TOC/TP within the Upper Kellwasser interval at those sites also rises distally (Perry Farm = 150, Irish Gulf = 194, Walnut Creek = 546) as TP declines exponentially (Tuite and Macko, 2013). TOC/TP among the Pando X-1 samples ranges from 419-1813 with a mean value of 1221. The relationship between the ratio of organic N to total P and TOC (Fig. 7B) suggests that increasing organic C preservation is correlated with a diminishing relative P abundance. Both cross-plots in Fig. 7 suggest that with respect to the biogeochemical processes that determine C/N/P relationships, there is significant continuity between the Appalachian and Madre de Dios Basins.

Sediment ratios of organic carbon (TOC) to total phosphorus (TP) and organic nitrogen (ON) provide an indication of the degree to which the macronutrients N and P have been remineralized in sediments relative to the C that was fixed by primary production and subsequently preserved in sedimentary organic matter. Although ON can be differentiated from total nitrogen (TN) based on the regression of TN against TOC (as in Fig. 7A) to quantify the contribution of clay-bound inorganic N to TN, TP is used as a proxy for organic P because detrital P is typically a minor component of TP in basinal settings (Algeo and Ingall, 2007). Modern green algae, including prasinophytes, exhibit a cellular C/N of  $\sim$ 6-8:1 and a C/P of ~200:1 (Quigg et al., 2003). Assuming that algal stoichiometry is an evolutionarily conservative trait (Quigg et al., 2003), the Devonian ancestors of this green algal clade were likely similar in their major element compositions. The TOC/ON ratio in the Pando X-1 samples, 44.5 (Fig. 7A), is 5–7 times the cellular C/N of green algal biomass, but likely overestimates the bioavailability of recycled N because an undetermined fraction of reactive N was removed from the system as N<sub>2</sub> via denitrification and/or Annamox and as NH<sub>4</sub><sup>+</sup> fixed within clay minerals. The mean TOC/TP ratio, 1221, is more

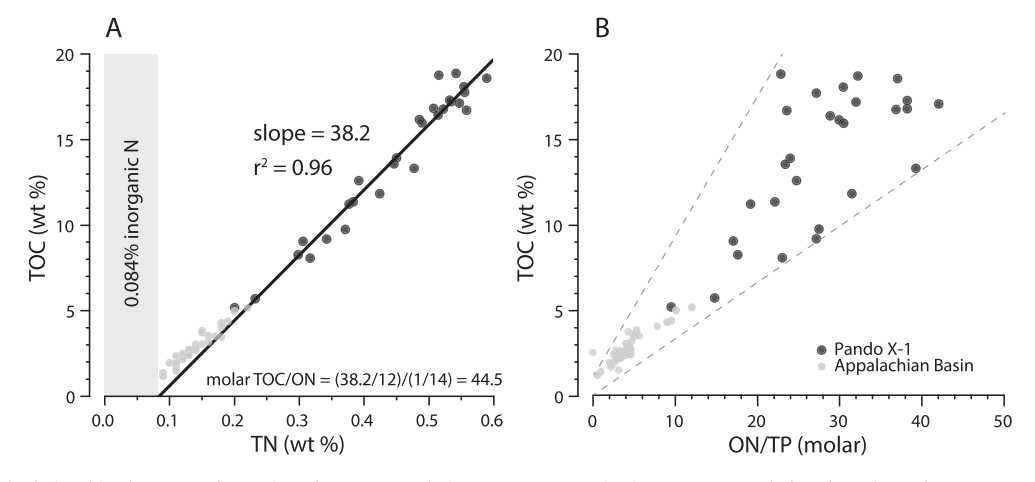


Fig. 7. C/N/P elemental relationships (TOC = total organic carbon, TN = total nitrogen, ON = organic nitrogen, TP = total phosphorus). Pando X-1 core samples are represented by black circles. Values for three Upper Kellwasser-equivalent intervals from the Appalachian Basin of western New York detailed in Tuite and Macko (2013) are represented by gray points. Regression line is for Pando samples only. (A) TOC and TN are highly correlated and the slope of the regression represents a very consistent ratio of organic C to organic N (TOC/ON) that is much greater than modern green algal biomass C/N (~8:1) (Quigg et al., 2003). The positive intercept on the TN axis is a result of the incorporation of a consistent mass of ammonium ion (NH<sub>4</sub><sup>+</sup>) in clay mineral matrices. That inorganic N (IN) component in all Pando samples is approximately 0.084% and is represented by the shaded area on the left. Organic N (ON) is calculated as the difference between TN and IN. (B) The positive relationship between ON/TP and TOC suggests that preferential regeneration of P versus N is correlated with greater organic C accumulation. Together, both cross-plots indicate the continuity of biogeochemical processes in the Appalachian and Madre de Dios basins.

than six times the cellular C/P ratio of green algae. Together, these ratios suggest that the upward diffusion of regenerated N and P in the forms of ammonium and phosphate were deficient in N relative to living biomass. A positive relationship between TOC and ON/TP (Fig. 7B) indicates that increasing organic C accumulation is correlated with increasing remineralization of P relative to N.

Because of the importance of recycled nutrients in sustaining production in shallow epeiric seas, the stoichiometrically unbalanced regeneration of P in favor of N suggests that primary production in the Madre de Dios Basin was chronically N-limited. C/N/P ratios suggest that primary production was also N-limited in the Appalachian Basin during deposition of the Upper Kellwasser interval and increased in severity with increasing distance from shore (Tuite and Macko, 2013). The development of forest ecosystems and intensified pedogenesis in the Late Devonian had a significant impact on the nutrient biogeochemistry of adjoining marine basins (Algeo and Scheckler, 1998; Tuite and Macko, 2013), On a timescale of ~10,000 years, the export of reactive N and P from new tropical forest soils to adjacent watersheds reverses dramatically from high P/low N to high N/low P (Hedin et al., 2003) as the P derived from weathered minerals becomes increasing occluded in plant-inaccessible forms (Walker and Syers, 1976) while bacterial N fixation and nitrate loss from soil leaching increase. Assuming a similar biogeochemistry in the Late Devonian, new forests likely became net exporters of reactive N to nearby epicontinental basins in a relatively brief geological timeframe. coccolithophores, rather than ameliorating N limitation in stratified epeiric seas, the augmentation of primary biomass and consequent heterotrophic O2 demand fueled by terrestrially derived N may have enhanced the remineralization of P via the anoxia/productivity feedback (Van Cappellen and Ingall, 1994), reinforcing the N-limitation of eukaryotic algae.

## 3.4.2. Isotopic nitrogen and carbon

With a single significant outlier, the range of  $\delta^{13}C_{org}$  values along the 20 m Pando X-1 interval is 0.8%. The sample at 1566.02 m is 0.8% more  $^{13}C_{-enriched}$  than the mean  $\delta^{13}C_{org}$  (Fig. 8). We propose that this excursion correlates with a positive 3% excursion observed in the earliest *triangularis* zone in the Upper Kellwasser sections of Kowala, Poland (Joachimski et al., 2001) and the Appalachian Basin (Murphy et al., 2000b). Even without a tightly constrained Frasnian/Famennian boundary, this isotopic excursion links the 28 samples analyzed from this interval to the Upper Kellwasser events at other localities, though more chemostratigraphic data is necessary for global correlation.

In the Appalachian Basin,  $\delta^{15}N_{total}$  values at Perry Farm, Irish Gulf, and Walnut Creek are very consistent:  $-0.2\% \pm 0.5$  (n=24),  $-0.1\% \pm 0.4$  (n=9), and  $-0.1 \pm 0.2$  (n=5), respectively (Tuite and Macko, 2013). Excluding the uppermost sample in the section, the mean  $\delta^{15}N_{total}$  value in the Pando X-1 samples is  $1.0\% \pm 0.3$  (n=27), a  $\delta^{15}N$  enrichment of  $\sim 1\%$  relative to the Appalachian Basin values. The uppermost sample is significantly more  $\delta^{15}N_{total}$ -enriched with a value of 3.8%. (Fig. 8).

The reservoir of reactive N in marine systems is continuously depleted by losses of organic N to burial and  $N_2$  to the atmosphere. Sources of new reactive N include N fixed in terrestrial soils that is transported by river discharge or atmospheric deposition, upwelling from deeper, nutrient-rich water, and in situ N fixation by diazotrophic prokaryotes. Although N-limitation may prompt N fixation, there are multiple physical and ecological barriers to ameliorating N-limitation via fixation including energetic constraints, limitation by other nutrients, and competition with non-fixing species (Vitousek and Howarth, 1991). Because of the high energetic cost required to rend triply bonded  $N_2$ , the small isotope fractionation associated with N fixation results in diazotrophic biomass  $\delta^{15}$ N that differs little from atmospheric  $\delta^{15}$ N (by definition,

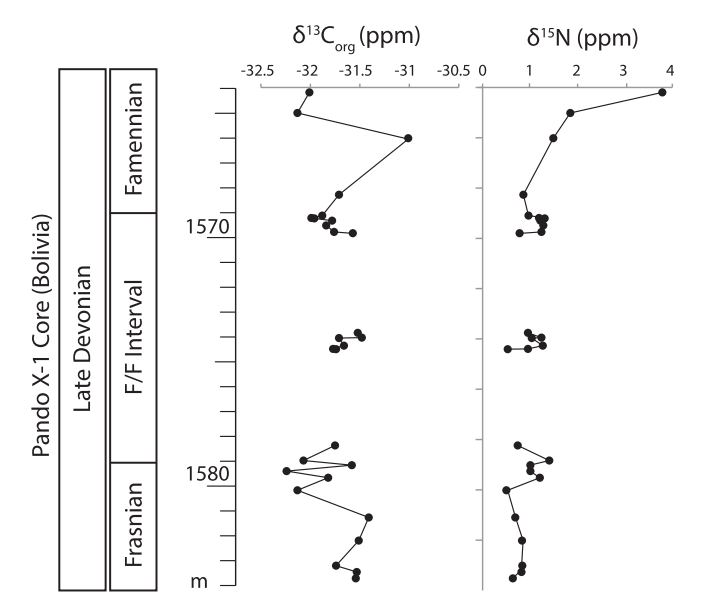


**Fig. 8.** Stable isotope stratigraphy  $(\delta^{13}C_{org}$  and  $\delta^{15}N_{total})$  for Pando X-1 core.  $\delta^{15}N_{total}$  values exhibit little variation (0 to +2%) with the exception of the uppermost sample which is significantly more  $^{15}N_{-}$ enriched (>+2.0%). Variation in  $\delta^{13}C_{org}$  values is likewise very limited. The sample at 1566.02 m, however, is 0.8% more  $^{13}C_{-}$ enriched than the mean  $\delta^{13}C_{org}$  and may correlate to a positive 3% excursion observed in the earliest *triangularis* zone in the Kowala Upper Kellwasser section in Poland.

 $\delta^{15}N_{air}$  = 0‰) (Macko et al., 1984; Minagawa and Wada, 1986) and is more depleted than modern sediment  $\delta^{15}N$  values that typically resemble the mean  $\delta^{15}N$  of marine nitrate (~+5‰) (Peters et al., 1978; Brandes and Devol, 2002; Robinson et al., 2012). The depleted  $\delta^{15}N$  values that are typical of organic-rich marine facies throughout the Phanerozoic have, therefore, often been interpreted as indicating periods of prokaryote-dominated phytoplankton communities (Rau et al., 1987; Sachs and Repeta, 1999; Kuypers et al., 2004; Meyers, 2006; Higgins et al., 2010). Our biomarker assemblages, however, point to biomass dominated by eukaryotic phytoplankton communities in association with depleted sediment  $\delta^{15}N$  values in both the Appalachian and Madre de Dios Basins.

There are several mechanisms that contribute to the depletion of sediment  $\delta^{15}N$  in low oxygen marine environments like those that obtained during the deposition of Late Devonian black shales. Where water column oxygen levels are sufficiently low to inhibit nitrification and the subsequent  $\delta^{15}N$  enrichment associated with denitrification, sediment  $\delta^{15}N$  will reflect the small fractionation associated with fixation of atmospheric N2 (Quan and Falkowski, 2009). The redox control of metal cofactors available for incorporation into nitrogenase, the enzyme that enables diazotrophic N fixation, is another mechanism that exerts an influence on sediment δ<sup>15</sup>N. Under low oxygen, reducing conditions Mo is rapidly scavenged from the water column and nitrogenases incorporate Fe and V in place of Mo. Fe and V nitrogenases, however, produce biomass that is 6-7‰ more depleted than (Mo)-nitrogenase (Zhang et al., 2014). Another mechanism has been observed in degrading algal biomass in laboratory experiments where residual biomass undergoes  $^{15}$ N depletion. Lehmann et al. (2002) observed a  $\sim 3\%$ depletion of algal  $\delta^{15}N$  during early diagenesis of dead algae under anoxic conditions. Finally, Higgins et al. (2012) proposed that the greater assimilation fractionation associated with NH<sub>4</sub><sup>+</sup> versus NO<sub>3</sub> uptake by eukaryotic algae resulted in <sup>15</sup>N-depleted biomass and sediment values where NH<sub>4</sub> was the dominant reactive N species (Higgins et al., 2012). The observation that sediment  $\delta^{15}$ N values resemble those of biomass produced by N fixation is, therefore, neither a necessary nor sufficient argument for a prokaryotedominated phytoplankton.

Ammonium was likely the dominant reactive N species in epeiric basins of the Late Devonian because oxidation of reduced N (nitrification) at the base of the photic zone would have been inhibited by persistent dysoxic conditions and precluded during rare episodes of euxinia. Thus, the upward diffusion of remineralized organic N in the form of ammonium was likely the primary source of reactive N in the photic zone, although diazotrophy and terrestrial N were likely important sources also in some locations. The demonstrated proclivity of prasinophytes for ammonium-rich environments (Prauss, 2007) supports a model for Devonian black shale microbial ecology in which eukaryotic algae dominate phytoplankton biomass even while sediment  $\delta^{15}N$  values preserve the isotopic signature of the small contribution of diazotrophic prokaryotes to overall planktonic biomass. In contrast to other intervals of Paleozoic time when  $C_{29}$  sterol-synthesizing green algal lineages like Chlorophyceae (Kodner et al., 2008) were the dominant eukaryotic phytoplankton (Grantham and Wakefield. 1988; Schwark and Empt, 2006), the reason why prasinophyte source contributions were so pronounced in the Late Devonian and other periods of apparent N-limitation is an interesting conundrum that is yet to be resolved.

The  ${\sim}1\%o$   $\delta^{15}N$  enrichment of the Pando X-1 samples with respect to contemporaneous Appalachian Basin samples may reflect latitudinal influences on coupled nitrification/denitrification. Cooler temperatures at high latitude may have increased  $O_2$  solubility thus deepening the surface mixed layer seasonally, permitting more oxidation of ammonium diffusing upward through the chemocline and subsequent loss of depleted  $N_2$  via denitrification near the base of the photic zone. Likewise, significant seasonal differences in solar insolation at high latitude may have diminished primary production and resulting heterotrophic respiration during winter months, permitting deeper penetration of oxic surface waters.

## 4. Conclusions

Detailed lipid biomarker stratigraphic records compiled for the Upper Kellwasser intervals for two different foreland epicontinental basins, from a low and high paleolatitude, indicated a stable marine microbial community, characterized by abundant eukaryotic phytoplankton, as indicated by low hopane/sterane ratios (consistently < 0.75). Consistently higher  $C_{28}/C_{29}$  sterane ratios in the Madre de Dios Basin (average of 0.52), coupled with palynological evidence for abundant *Tasmanites* and *Leiosphaeridia* cysts in these rocks, suggest that prasinophyte algae were the more abundant primary producers in the nutrient-replete marine conditions at high paleolatitude compared with the lower latitude setting. C/N/P elemental relationships suggest intense remineralization of organic N and P as well as chronic N-limitation of primary production that was not ameliorated by N fixation.

The extremely low absolute abundances of Chlorobi-derived aromatic carotenoids (aryl isoprenoids and C<sub>40</sub> compounds) detected for the Upper Kellwasser black shales from the Appalachian Basin, together with other complementary chemostratigraphic redox proxies (Murphy et al., 2000a), suggests marine redox conditions where sulfidic waters were largely restricted to the lower water column. Despite the high TOC contents of rocks from the Madre de Dios Basin core and likely sulfidic conditions in deep waters, low abundances of aromatic carotenoid markers detected in the Pando X-1 core suggest that suitable niche space for Chlorobi may only have been sustainable in the summer when solar insolation was intense enough to deepen the lower photic zone to the euxinic water column. Completely unraveling the basinal redox models, however, will require integrating the biomarker

stratigraphic records with independent data from paleontology and inorganic geochemistry, which is the subject of future study.

While biomarker assemblages show diagnostic characteristics observed previously for Late Devonian rocks and oils, persistent differences for certain biomarker distributions (including  $C_{28}/C_{29}$  sterane ratios, tricyclic terpane/hopane ratio and methylhopane indices) between the high and low paleolatitude basins highlights the caution that must be employed when extrapolating the pale-oenvironmental conditions of any particular basin to global ocean models. Heterogeneity in nutrient availability, local environmental conditions, and the biota that these support is expected within a global ocean system for any interval of Earth history.

## Acknowledgments

This work was funded principally by a National Science Foundation Earth Sciences Program grants to GDL (NSF-EAR 1348988) and DLB (NSF-EAR 1348981). GDL also thanks the Agouron Institute for grant support. EEH acknowledges graduate student support from the NSF GRFP, AAPG, SEPM, the Gulf Coast Section of SEPM, and the Paleontological Society. The authors are indebted to Sarah de la Rue for providing Pando X-1 core samples for geochemical analysis.

## Associate Editor-Kliti Grice

#### References

Algeo, T.J., Ingall, E., 2007. Sedimentary C<sub>org</sub>. P ratios, paleocean ventilation, and Phanerozoic atmospheric pO<sub>2</sub>. Palaeogeography, Palaeoclimatology, Palaeoecology 256, 130–155.

Algeo, T.J., Scheckler, S.E., 1998. Terrestrial-marine teleconnections in the Devonian: links between the evolution of land plants, weathering processes, and marine anoxic events. Philosophical Transactions of the Royal Society of London B 353, 113–130.

Alroy, J., 2008. Dynamics of origination and extinction in the marine fossil record. Proceedings of the National academy of Sciences of the United States of America 105, 11536–11542.

Aquino Neto, F.R., Trigüis, J., Azevedo, D.A., Rodrigues, R., Simoneit, B.R.T., 1992. Organic geochemistry of geographically unrelated tasmanites. Organic Geochemistry 18, 791–803.

Arthur, M.A., Sageman, B.B., 1994. Marine black shales: depositional mechanisms and environments of ancient deposits. Annual Review of Earth and Planetary Sciences 22, 499–551.

Aspila, K.I., Agemian, H., Chau, A.S.Y., 1976. A semi-automated method for the determination of inorganic, organic and total phosphate in sediments. Analyst 101, 187–197.

Averbuch, O., Tribovillard, N., Devleeschouwer, X., Riquier, L., Mistiaen, B., van Vliet-Lanoe, B., 2005. Mountain building-enhanced continental weathering and organic carbon burial as major causes for climatic cooling at the Frasnian-Famennian boundary (c. 376 Ma)? Terra Nova 17, 25–34.

Baird, G.C., Brett, C.E., Ver Straeten, C.A., 1999. The First Great Devonian Flooding Episodes in Western New York: Reexamination of Union Springs, Oatka Creek and Skaneateles Formation Successions (Latest Eifelian–Lower Givetian) in the Buffalo-Seneca Lake Region, vol. 71. New York State Geological Association Field Trip Guide Book, pp. 1–444.

Bambach, R.K., 2006. Phanerozoic biodiversity mass extinctions. The Annual Review of Earth and Planetary Science 34, 127–155.

Bambach, R.K., Knoll, A.H., Wang, S.C., 2004. Origination, extinction, and mass depletions of marine diversity. Paleobiology 30, 522–542.

Becker, R.T., House, M.R., 1994. Kellwasser events and goniatite successions in the Devonian of the Montagne Noire with comments on possible causations. Courier-Forschung-Institut Senckenberg 16, 45–77.

Bond, D., Wignall, P.B., Racki, G., 2004. Extent and duration of marine anoxia during the Frasnian–Famennian (Late Devonian) mass extinction in Poland, Germany, Austria and France. Geological Magazine 141, 173–193.

Boyer, D.L., Droser, M.L., 2011. A combined trace- and body-fossil approach reveals high-resolution record of oxygen fluctuations in Devonian seas. Palaios 26, 500-

Boyer, D.L., Owens, J.D., Lyons, T.W., Droser, M.L., 2011. Joining forces: combined biological and geochemical proxies reveal a complex but refined high-resolution palaeo-oxygen history in Devonian epeiric seas. Palaeogeography, Palaeoclimatology, Palaeoecology 308, 134–146.

Brandes, J.A., Devol, A.H., 2002. A global marine-fixed nitrogen isotopic budget: implications for Holocene nitrogen cycling. Global Biogeochemical Cycles 16, 67-1-67-14.

- Brett, C.E., Dick, V.B., Baird, G.C., 1991. Comparative taphonomy and paleoecology of Middle Devonian dark gray and black shale facies from western New York. In: Landing, E., Brett, C.E. (Eds.), Dynamic Stratigraphy and Depositional Environments of the Hamilton Group (Middle Devonian) in New York State, Part II. Bulletin. New York State Museum, pp. 5–36.
- Brown, T.C., Kenig, F., 2004. Water column structure during deposition of Middle Devonian–Lower Mississippian black and green/gray shales of the Illinois and Michigan Basins: a biomarker approach. Palaeogeography, Palaeoclimatology, Palaeoecology 215, 59–85.
- Buggisch, W., 1991. The global Frasnian/Famennian "Kellwasser Event". Geologische Rundschau 80, 49–72.
- Calvert, S.E., 2004. Beware intercepts: interpreting compositional ratios in multicomponent sediments and sedimentary rocks. Organic Geochemistry 35, 981– 987.
- Cao, C., Love, G.D., Hays, L.E., Bowring, S.A., Wang, W., Shen, S., Summons, R.E., 2009. Biogeochemical evidence for euxinic oceans and ecological disturbance presaging the end Permian Mass Extinction Event. Earth and Planetary Science Letters 281, 188–201.
- Clifford, D.J., Clayton, J.L., Sinninghe Damsté, J.S., 1998. 2,3,6-/3,4,5-Trimethyl substituted diaryl carotenoid derivatives (Chlorobiaceae) in petroleums of the Belarussian Pripyat River Basin. Organic Geochemistry 29, 1253–1267.
- Coplen, T.B., Brand, W.A., Gehre, M., Groning, M., Meijer, H.A.J., Toman, B., Verkouteren, R.M., 2006. New guidelines for  $\delta^{13}$ C measurements. Analytical Chemistry 78, 2439–2441.
- De la Rue, S.R., 2010. Implications for an Anoxia-related Control on Green Algal Distributions at the Late Devonian Frasnian/Famennian Boundary (Doctoral dissertation). University of Idaho.
- Doughty, D.M., Hunter, R.C., Summons, R.E., Newman, D.K., 2009. 2-Methylhopanoids are maximally produced in akinetes of *Nostoc punctiforme*: geobiological implications. Geobiology 7, 524–532.
- Droser, M.L., Bottjer, D.J., Sheehan, P.M., McGhee Jr., G.R., 2000. Decoupling of taxonomic and ecologic severity of Phanerozoic marine mass extinctions. Geology 28, 675–678.
- Dumitrescu, M., Brassell, S.C., 2005. Biogeochemical assessment of sources of organic matter and paleoproductivity during the early Aptian Oceanic Anoxic Event at Shatsky Rise, ODP Leg 198. Organic Geochemistry 36, 1002–1022.
- Dutta, S., Greenwood, P.F., Brocke, R., Schaefer, R.G., Mann, U., 2006. New insights into the relationship between *Tasmanites* and tricyclic terpenoids. Organic Geochemistry 37, 117–127.
- Farrimond, P., Talbot, H.M., Watson, D.F., Schulz, L.K., Wilhelms, A., 2004. Methylhopanoids: molecular indicators of ancient bacteria and a petroleum correlation tool. Geochimica et Cosmochimica Acta 68, 3873–3882.
- French, K.L., Rocher, D., Zumberge, J.E., Summons, R.E., 2015. Assessing the distribution of sedimentary C<sub>40</sub> carotenoids through time. Geobiology 13, 139–151.
- Golonka, J., Ross, M.I., Scotese, C.R., 1994. Phanerozoic paleogeographic and paleoclimatic modeling maps. In: Embry, A.F., Beauchamp, B., Glass, D.J. (Eds.), Pangea: Global Environments and Resources Memoir 17. Canadian Society of Petroleum Geology, pp. 1–47.
- Grantham, P.J., Wakefield, L.L., 1988. Variations in the sterane carbon number pattern distributions of marine source rock derived crude oils through geological times. Organic Geochemistry 12, 61–77.
- Greenwood, P.F., Arouri, K.R., George, S.C., 2000. Tricyclic terpenoids composition of Tasmanites kerogen as determined by pyrolysis GC-MS. Geochimica et Cosmochimica Acta 64, 1249–1263.
- Grice, K., Cao, C., Love, G.D., Böttcher, M.E., Twitchett, R.J., Grosjean, E., Summons, R. E., Turgeon, S.C., Dunning, W., Jin, Y., 2005. Photic zone euxinia during the Permian-Triassic superanoxic event. Science 307, 706–709.
- Harris, N.B., 2005. The Deposition of Organic-carbon-rich Sediments: Models, Mechanisms, and Consequences, vol. 82. The Society for Sedimentary Geology (SEPM) Special Publication, pp. 1–5.
- Hartgers, W.A., Sinninghe Damsté, J.S., Requejo, A.G., Allan, J., Hayes, J.M., Ling, Y., Xie, T.-M., Primack, J., de Leeuw, J.W., 1994. A molecular and carbon isotopic study towards the origin and diagenetic fate of diaromatic carotenoids. Organic Geochemistry 22, 703–725.
- Hedin, L.O., Vitousek, P.M., Matson, P.A., 2003. Nutrient losses over four million years of tropical forest development. Ecology 84, 2231–2255.
- Higgins, M.B., Robinson, R.S., Carter, S.J., Pearson, A., 2010. Evidence from chlorin nitrogen isotopes for alternating nutrient regimes in the Eastern Mediterranean Sea. Earth and Planetary Science Letters 290, 102–107.
- Higgins, M.B., Robinson, R.S., Husson, J.M., Carter, S.J., Pearson, A., 2012. Dominant eukaryotic export production during ocean anoxic events reflects the importance of recycled NH<sub>4</sub>\*. Proceedings of the National academy of Sciences of the United States of America 109, 2269–2274.
- House, M.R., 2002. Strength, timing, setting and cause of mid-Palaeozoic extinctions. Palaeogeography, Palaeoclimatology, Palaeoecology 181, 5–25.
- Huang, W.-Y., Meinschein, W.G., 1979. Sterols as ecological indicators. Geochimica et Cosmochimica Acta 43, 739–745.
- Joachimski, M.M., Buggisch, W., 1993. Anoxic events in the late Frasnian: causes of the Frasnian Famennian faunal crisis? Geology 21, 675–678.
- Joachimski, M.M., Ostertag-Henning, C., Pancost, R.D., Strauss, H., Freeman, K.H., Littke, R., Sinninghe Damsté, J.S., Racki, G., 2001. Water column anoxia, enhanced productivity and concomitant changes in δ<sup>13</sup>C and δ<sup>34</sup>S across the Frasnian-Famennian boundary (Kowala – Holy Cross Mountains, Poland). Chemical Geology 175, 109–131.

- Kirchgasser, W.T., Baird, G.C., Brett, C.E., 1988. Regional placement of Middle/Upper Devonian (Givetian-Frasnian) boundary in western New York State. In: McMillan, N.J., Embry, A.F., Glass, D.J. (Eds.), Devonian of the World Memoir 14. Canadian Society of Petroleum Geologists, pp. 113–117.
- Kodner, R.B., Pearson, A., Summons, R.E., Knoll, A.H., 2008. Sterols in red and green algae: quantification, phylogeny, and relevance for the interpretation of geologic steranes. Geobiology 6, 411–420.
- Koopmans, M.P., Rijpstra, W.I.C., Klapwijk, M.M., de Leeuw, J.W., Lewan, M.D., Sinninghe Damsté, J.S., 1999. A thermal and chemical degradation approach to decipher pristane and phytane precursors in sedimentary organic matter. Organic Geochemistry 30, 1089–1104.
- Kuypers, M.M.M., Van Breugel, Y., Schouten, S., Erba, E., Sinninghe Damsté, J.S., 2004. N<sub>2</sub>-fixing cyanobacteria supplied nutrient N for Cretaceous oceanic anoxic events. Geology 32, 853–856.
- LaPorte, D.F., Holmden, C., Patterson, W.P., Loxton, J.D., Melchin, M.J., Mitchell, C.E., Finney, S.C., Sheets, H.D., 2009. Local and global perspectives on carbon and nitrogen cycling during the Hirnantian glaciation. Palaeogeography, Palaeoclimatology, Palaeoecology 276, 182–195.
- Lehmann, M.F., Bernasconi, S.M., Barbieri, A., McKenzie, J.A., 2002. Preservation of organic matter and alteration of its carbon and nitrogen isotope composition during simulated and in situ early sedimentary diagenesis. Geochimica et Cosmochimica Acta 66, 3573–3584.
- Lenniger, M., Nøhr-Hansen, H., Hills, L.V., Bjerrum, C.J., 2014. Arctic black shale formation during Cretaceous Oceanic Anoxic Event 2. Geology 42, 799–802.
- Levman, B.G., Von Bitter, P.H., 2002. The Frasnian-Famennian (mid-Late Devonian) boundary in the type section of the Long Rapids Formation, James Bay Lowlands, northern Ontario, Canada. Canadian Journal of Earth Sciences 39, 1795–1818.
- Macko, S.A., Entzeroth, L., Parker, P.L., 1984. Regional differences in nitrogen and carbon isotopes on the continental-shelf of the Gulf of Mexico. Naturwissenschaften 71, 374–375.
- Marynowski, L., Filipiak, P., 2007. Water column euxinia and wildfire evidence during deposition of the Upper Famennian Hangenberg event horizon from the Holy Cross Mountains (central Poland). Geological Magazine 144, 569–595.
- Marynowski, L., Rakociński, M., Zatoń, M., 2007. Middle Famennian (Late Devonian) interval with pyritized fauna from the Holy Cross Mountains (Poland): organic geochemistry and pyrite framboid diameter study. Geochemical Journal 41, 187–200.
- Marynowski, L., Filipiak, P., Zatoń, M., 2010. Geochemical and palynological study of the Upper Famennian Dasberg event horizon from the Holy Cross Mountains (central Poland). Geological Magazine 147, 527–550.
- Marynowski, L., Rakociński, M., Borcuch, E., Kremer, B., Schubert, B.A., Jahren, A.H., 2011. Molecular and petrographic indicators of redox conditions and bacterial communities after the F/F mass extinction (Kowala, Holy Cross Mountains, Poland). Palaeogeography, Palaeoclimatology, Palaeoecology 306, 1–14.
- Maslen, E., Grice, K., Gale, J.D., Hallmann, C., Horsfield, B., 2009. Crocetane: a potential marker of photic zone euxinia in thermally mature sediments and crude oils of Devonian age. Organic Geochemistry 40, 1–11.
- McGhee Jr., G.R., 1996. The Late Devonian Mass Extinction: The Frasnian/Famennian Crisis. Columbia University Press, New York.
- Melendez, I., Grice, K., Trinajstic, K., Ladjavardi, M., Greenwood, P., Thompson, K., 2013a. Biomarkers reveal the role of photic zone euxinia in exceptional fossil preservation: an organic geochemical perspective. Geology 41, 123–126.
- Melendez, I., Grice, K., Schwark, L., 2013b. Exceptional preservation of Palaeozoic steroids in a diagenetic continuum. Scientific Reports 3 (article number 2768).
- Meyers, P.A., 2006. Paleoceanographic and paleoclimatic similarities between Mediterranean sapropels and Cretaceous black shales. Palaeogeography, Palaeoclimatology, Palaeoecology 235, 305–320.
- Minagawa, M., Wada, E., 1986. Nitrogen isotope ratios of red tide organisms in the East-China-Sea a characterization of biological nitrogen-fixation. Marine Chemistry 19, 245–259.
- Müller, P.J., 1977. C-N ratios in Pacific deep-sea sediments effect of inorganic ammonium and organic nitrogen-compounds sorbed by clays. Geochimica et Cosmochimica Acta 41, 765–776.
- Murphy, A.E., Sageman, B.B., Hollander, D.J., Lyons, T.W., Brett, C.E., 2000a. Black shale deposition and faunal overturn in the Devonian Appalachian basin: clastic starvation, seasonal water-column mixing, and efficient biolimiting nutrient recycling. Paleoceanography 15, 280–291.
- Murphy, A.E., Sageman, B.B., Hollander, D.J., 2000b. Eutrophication by decoupling of the marine biogeochemical cycles of C, N, and P: a mechanism for the Late Devonian mass extinction. Geology 28, 427–430.
- Over, D.J., 1997. Conodont biostratigraphy of the Java Formation (Upper Devonian) and the Frasnian–Famennian boundary in western New York State. Geological Society of America Special Paper 321, 161–177.
- Over, D.J., 2002. The Frasnian–Famennian boundary in central and eastern United States. Palaeogeography, Palaeoclimatology, Palaeoecology 181, 153–169.
- Over, D.J., De la Rue, S., Isaacson, P., Ellwood, B., 2009. Upper Devonian conodonts from black shales of the high latitude Tomachi Formation, Madre de Dios Basin, northern Bolivia. Palaeontographica Americana 62, 89–99.
- Over, D.J., Baird, G.C., Kirchgasser, W.T., 2013. Middle-Upper Devonian strata along the Lake Erie Shore, Western New York. New York State Geological Association Field Trip Guidebook, 85th Annual Meeting, 182–219.
- Peters, K.E., Sweeney, R.E., Kaplan, I.R., 1978. Correlation of carbon and nitrogen stable isotope ratios in sedimentary organic-matter. Limnology and Oceanography 23, 598–604.

- Peters, K.E., Wagner, J.B., Carpenter, D.G., Conrad, K.T., 1997a. World class Devonian potential seen in eastern Madre de Dios basin. Part I. Oil & Gas Journal 95, 61–65.
- Peters, K.E., Wagner, J.B., Carpenter, D.G., Conrad, K.T., 1997b. World class Devonian potential seen in eastern Madre de Dios basin. Part II. Oil & Gas Journal 95, 84–87.
- Peters, K.E., Walters, C.C., Moldowan, J.M., 2005. Petroleum systems through time: Devonian Source Rocks. In: Peters, K.E., Walters, C.C., Moldowan, J.M. (Eds.), The Biomarker Guide: Biomarkers and Isotopes in Petroleum Exploration and Earth History, vol. 2. Cambridge University Press, Cambridge, pp. 794–807.
- Prauss, M.L., 2007. Availability of reduced nitrogen chemospecies in photic-zone waters as the ultimate cause for fossil prasinophyte prosperity. Palaios 22, 489– 499.
- Quan, T.M., Falkowski, P.G., 2009. Redox control of N:P ratios in aquatic ecosystems. Geobiology 7, 124–139.
- Quigg, A., Finkel, Z.V., Irwin, A.J., Rosenthal, Y., Ho, T.Y., Reinfelder, J.R., Schofield, O., Morel, F.M.M., Falkowski, P.G., 2003. The evolutionary inheritance of elemental stoichiometry in marine phytoplankton. Nature 425, 291–294.
- Rashby, S.E., Sessions, A.L., Summons, R.E., Newman, D.K., 2007. Biosynthesis of 2-methylbacteriohopanepolyols by an anoxygenic phototroph. Proceedings of the National academy of Sciences of the United States of America 104, 15099–15104.
- Rau, G.H., Arthur, M.A., Dean, W.E., 1987. <sup>15</sup>N/<sup>14</sup>N variations in Cretaceous Atlantic sedimentary sequences implication for past changes in marine nitrogen biogeochemistry. Earth and Planetary Science Letters 82, 269–279.
- Raup, D.M., Sepkoski Jr., J.J., 1982. Mass extinctions in the marine fossil record. Science 215, 1501–1503.
- Revill, A.T., Volkman, J.K., O'Leary, T., Summons, R.E., Boreham, C.J., Banks, M.R., Denwar, K., 1994. Hydrocarbon biomarkers, thermal maturity, and depositional setting of tasmanite oil shales from Tasmania, Australia. Geochimica et Cosmochimica Acta 58, 3803–3822.
- Rivera, K.T., Puckette, J., Quan, T.M., 2015. Evaluation of redox versus thermal maturity controls on δ<sup>15</sup>N in organic rich shales: a case study of the Woodford Shale, Anadarko Basin, Oklahoma, USA. Organic Geochemistry 83, 127–139.
- Robinson, R.S., Kienast, M., Albuquerque, A.L., Altabet, M., Contreras, S., Holz, R.D., Dubois, N., Francois, R., Galbraith, E., Hsu, T.C., Ivanochko, T., Jaccard, S., Kao, S.J., Kiefer, T., Kienast, S., Lehmann, M.F., Martinez, P., McCarthy, M., Mobius, J., Pedersen, T., Quan, T.M., Ryabenko, E., Schmittner, A., Schneider, R., Schneider-Mor, A., Shigemitsu, M., Sinclair, D., Somes, C., Studer, A., Thunell, R., Yang, J.Y., 2012. A review of nitrogen isotopic alteration in marine sediments. Paleoceanography 27, PA4203.
- Rohrssen, M., Love, G., Fisher, W., Finnegan, S., Fike, D.A., 2013. Lipid biomarkers record fundamental changes in microbial community structure of tropical seas during the Late Ordovician Hirnantian Glaciation. Geology 41, 127–130.
- Rohrssen, M., Gill, B.C., Love, G.D., 2015. Scarcity of the  $C_{30}$  sterane biomarker, 24-n-propylcholestane, in Lower Paleozoic marine paleoenvironments. Organic Geochemistry 80, 1–7.
- Sachs, J.P., Repeta, D.J., 1999. Oligotrophy and nitrogen fixation during eastern Mediterranean sapropel events. Science 286, 2485–2488.
- Sageman, B.B., Murphy, A.E., Werne, J.P., ver Straeten, C.A., Hollander, D.J., Lyons, T. W., 2003. A tale of shales: the relative roles of production, decomposition, and dilution in the accumulation of organic-rich strata, Middle-Upper Devonian, Appalachian Basin. Chemical Geology 195, 229–273.
- Schieber, J., Baird, G., 2001. On the origin and significance of pyrite spheres in Devonian black shales of North America. Journal of Sedimentary Research 71, 155–166.
- Schwark, L., Empt, P., 2006. Sterane biomarkers as indicators of Palaeozoic algal evolution. Palaeogeography, Palaeoclimatology, Palaeoecology 240, 225–236.

- Schwark, L., Frimmel, A., 2004. Chemostratigraphy of the Posidonia Black Shale, SW-Germany II. Assessment of extent and persistence of photic-zone anoxia using aryl isoprenoid distributions. Chemical Geology 206, 231–248.
- Scotese, C.R., McKerrow, W.S., 1990. Revised World maps and introduction. In: McKerrow, W.S., Scotese, C.R. (Eds.), Palaeozoic Palaeogeography and Biogeography. Geological Society Memoir 12, pp. 1–21.
- Simoneit, B.R.T., Leif, R.N., 1990. On the presence of tricyclic terpane hydrocarbons in Permian Tasmanite algae. Naturwissenschaften 77, 380–383.
- Summons, R.E., Powell, T.G., 1986. Chlorobiaceae in Palaeozoic seas combined evidence from biological markers, isotopes and geology. Nature 319, 763–765.
- Summons, R.E., Powell, T.G., 1987. Identification of aryl isoprenoids in source rocks and crude oils: biological markers for the green sulphur bacteria. Geochimica et Cosmochimica Acta 51, 557–566.
- Summons, R.E., Jahnke, L.L., Hope, J.M., Logan, G.A., 1999. 2-Methylhopanoids as biomarkers for cyanobacterial oxygenic photosynthesis. Nature 400, 554–557.
- Swezey, C.S., 2002. Regional stratigraphy and petroleum systems of the Appalachian Basin, North America. United States Geological Survey, Geologic Investigations Series, Map I-2768.
- Thayer, C.W., 1974. Marine paleoecology in the Upper Devonian of New York. Lethaia 7, 121–155.
- Tuite Jr., M.L., Macko, S.A., 2013. Basinward nitrogen limitation demonstrates role of terrestrial nitrogen and redox control of  $\delta^{15}N$  in a Late Devonian black shale. Geology 41, 1079–1082.
- Tyson, R.V., 2005. The "Productivity Versus Preservation" Controversy: Cause, Flaws, and Resolution, vol. 82. The Society for Sedimentary Geology (SEPM) Special Publication, pp. 17–33.
- Tyson, R.V., Pearson, T.H., 1991. Modern and ancient continental shelf anoxia: an overview. In: Tyson, R.V., Pearson, T.H. (Eds.), Modern and Ancient Continental Shelf Anoxia. Geological Society Special Publication, pp. 1–26.
- Van Cappellen, P., Ingall, E.D., 1994. Benthic phosphorus regeneration, net primary production, and ocean anoxia a model of the coupled marine biogeochemical cycles of carbon and phosphorus. Paleoceanography 9, 677–692.
- Van Helmond, N.A.G.M., Sluijs, A., Sinninghe Damsté, J.S., Reichart, G.-J., Voigt, S., Erbacher, J., Pross, J., Brinkhuis, H., 2015. Freshwater discharge controlled deposition of Cenomanian-Turonian black shales on the NW European epicontinental shelf (Wunstorf, northern Germany). Climate of the Past 11, 495–508.
- Vitousek, P.M., Howarth, R.W., 1991. Nitrogen limitation on land and in the sea how can it occur? Biogeochemistry 13, 87–115.
- Volkman, J.K., 2003. Sterols in microorganisms. Applied Microbiology and Biotechnology 60, 495–506.
- Volkman, J.K., Barrett, S.M., Dunstan, G.A., Jeffrey, S.W., 1994. Sterol biomarkers for microalgae from the green algal class Prasinophyceae. Organic Geochemistry 21, 1211–1218.
- Walker, T.W., Syers, J.K., 1976. Fate of phosphorus during pedogenesis. Geoderma 15, 1–19.
- Welander, P.V., Coleman, M.L., Sessions, A.L., Summons, R.E., Newman, D.K., 2010. Identification of a methylase required for 2-methylhopanoid production and implications the interpretation of sedimentary hopanes. Proceedings of the National academy of Sciences of the United States of America 107, 8537–8542.
- Woodrow, D.L., Isley, A.M., 1983. Facies, topography, and sedimentary processes in the Catskill Sea (Devonian), New York and Pennsylvania. Geological Society of America Bulletin 4, 459–470.
- Zhang, X.N., Sigman, D.M., Morel, F.M.M., Kraepiel, A.M.L., 2014. Nitrogen isotope fractionation by alternative nitrogenases and past ocean anoxia. Proceedings of the National academy of Sciences of the United States of America 111, 4782– 4787.